2-1-1991

Electron-bean biased reactive evaporation of silicon, silicon oxides, and silicon nitrides

Jen-Yu Yeh

Electron-Beam Biased Reactive Evaporation Of Silicon, Silicon Oxides, And Silicon Nitrides

Jen-Yu Yeh

February, 1991

THESIS

Submitted in Partial Fulfillment of the Requirements for
The Degree of Master of Science

APPROVED:

4/8/91
Dr. V. Lindberg, Thesis Advisor

4/8/91
Dr. P. Cardegna, Program Director,
Materials Science & Engineering

4/8/91
Dr. A. Entenberg, Thesis Committee

Rochester Institute of Technology
Rochester, New York 14623
Materials Science and Engineering

Electron-Beam Biased Reactive Evaporation Of Silicon, Silicon Oxides, And Silicon Nitrides

Jen-Yu Yeh

February, 1991

THESIS

Submitted in Partial Fulfillment of the Requirements for
The Degree of Master of Science

_____ 4-16-1991

Signature Date

ABSTRACT

Silicon and silicon related films were deposited onto glass slides and silicon wafers by electron-beam evaporation of silicon in oxygen and nitrogen atmospheres. An ionizer consisting of a heated tungsten wire biased with a negative voltage enhanced the opportunity of reactive deposition. Substrate temperature, chamber pressure, deposition rate, and biasing voltage were the controlled variables. The film reactive indices were measured using spectro-photometry and ellipsometry to examine the effects of these four variables. The refractive index obtained from silicon films is 4.18~4.42 and the refractive indices for silicon oxides range from 1.57 to 3.93. No evidence of silicon nitride formation was found. Statistics analyses of the results suggest chamber pressure and deposition rate are equally important factors in changing the refractive index. Biasing voltage has less effect. To produce the lowest refractive index, the rate must be as low as possible (less than 5 Å/s), oxygen pressure must be high (2×10^{-4} Torr), while electrical biasing must exist. Changing the biasing from 100 V to 500 V has little effect on refractive index.

Table of Contents

List of Figures

List of Tables

Acknowledgements

I wish to express my gratitude to Dr. Vern Lindberg, my advisor, Dr. Robert Clark, the Director of the Center for Materials Science and Engineering, and Dr. Peter Cardegna, the Director of the Program for Materials Science and Engineering at Rochester Institute of Technology.

I also owe thanks to the members of the Thin Films Lab, Bill Van Derveer, for helping me with the set up and maintenence of all instruments, T.S. Chen for teaching me the operation of instruments. Thanks also to CVC Corporation and the RIT Chemistry Department for their kind assistance in ellipsometry and FTIR.

Finally, yet most importantly, I would like to thank my family, for their love, support and understanding.

I. INTRODUCTION

IA. Function Of Optical Thin Films

The optical thin films I made are silicon, silicon oxides and silicon nitrides. With only one pump-down, a high-refractive-index silicon film and a low-refractive-index silicon oxide or silicon nitride film could be deposited simply by varying the reactive gases during deposition. A wide range of refractive indices are desirable in order to produce effective optical coatings such as antireflection coatings and high reflection coatings.

The performance of optical thin films results from the interference of light waves. The superposition of the incident wave and those waves reflected from each interface (film-film or film-substrate interfaces) will determine the resultant transmittance and reflectance[1]. As shown in Figure 1, some light is reflected and some is transmitted at each interface. The reflectance at an interface can be calculated with the Fresnel Formulae[2-7]. The reflectance and transmittance for the coated substrate will be modified from that of the uncoated substrate. The number of layers, refractive indices of the films and substrate, thickness of the films, and angle of incidence are the intrinsic variables which will affect the function of optical filters. The performance of a filter will vary at different wavelengths[1].

A thin film of refractive index n has both a physical thickness, d, and an optical thickness, nd. The optical thickness takes into account the change of wavelength in a medium, and hence we can always deal with the wavelength of light in vacuum. In most design cases a design wavelength is chosen, and optical thicknesses are given as a fraction of the design wavelength. Thus an optical thickness of a quarter -wavelength at a design wavelength λ corresponds to $nd = \lambda/4$.

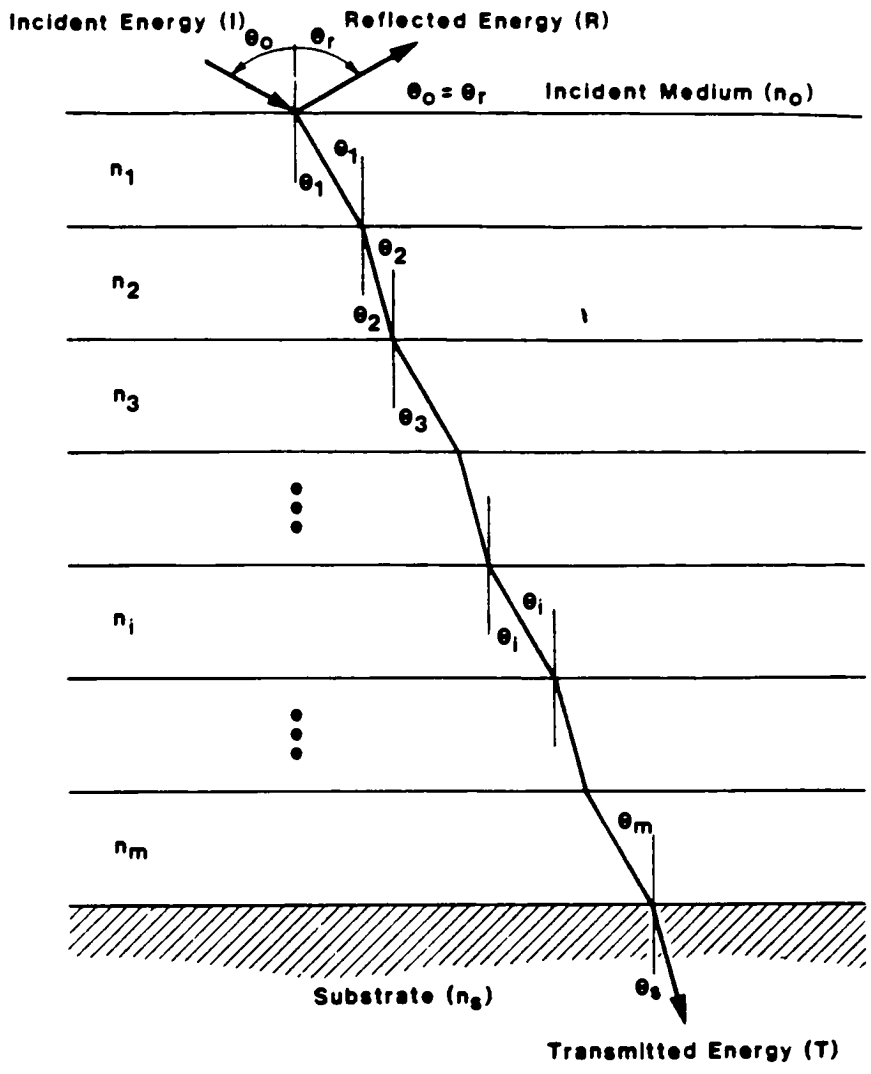

Figure 1 Reflectance, R, and transmittance, T, for light incident on an optical filter with the structure of a thin film stack. The index of refraction is n, and the layers are numbered starting from the incident medium[1].

All antireflection coatings have one characteristic: within a specific wavelength range, the reflectance is very small, ideally zero. The simplest antireflection coating can be achieved by the deposition a quarter-wave optical thickness, dielectric coating on the substrate. Results for MgF_2 on glass at different polarizations and angles of

incidence are given in Figure 2. The ideal characteristics for an antireflection device are:

(i) Large transmittance band width.

(ii) Low maximum reflectance[9].

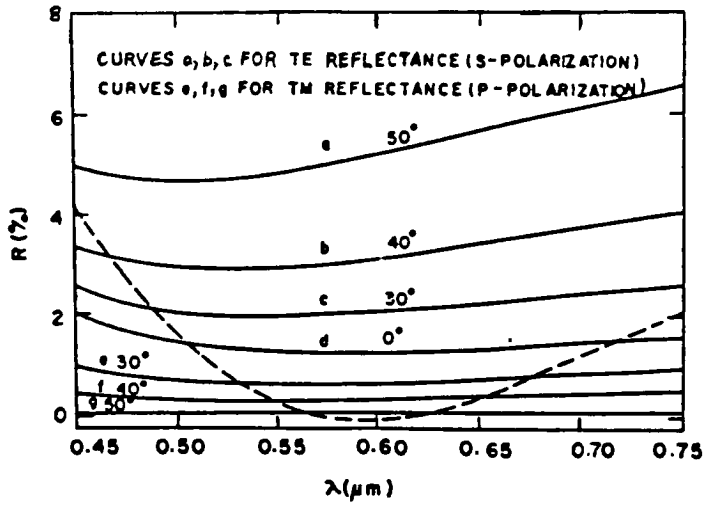

Figure 2. Reflectance versus wavelength for a quarter-wave (at 0.6 μm) antireflection coating of MgF_2 on glass (n1 = 1.38, ns = 1.52) at various angles of incidence. Also for comparison is shown (dotted) the reflectance curve for a quarter-quarter double-layer AR coating [n_1 = 1.38 (MgF_2), n_2 = 1.70 (SiO), ns =1.52 (glass)]. Figure taken from reference 8.

High reflectance coatings have a wavelength range where $R \approx 1$ and $T \approx 0$. High reflectance coatings can be achieved by alternating quarter-wave layers of high (H) and low (L) refractive index dielectric layers on a substrate. The structure is $H(LH)^p$ for a (2p+1) layer structure For this kind of device, there should be a wide range of constant reflectance[8] as is shown in Figure 3.

Details of these two devices will be discussed in the theory section.

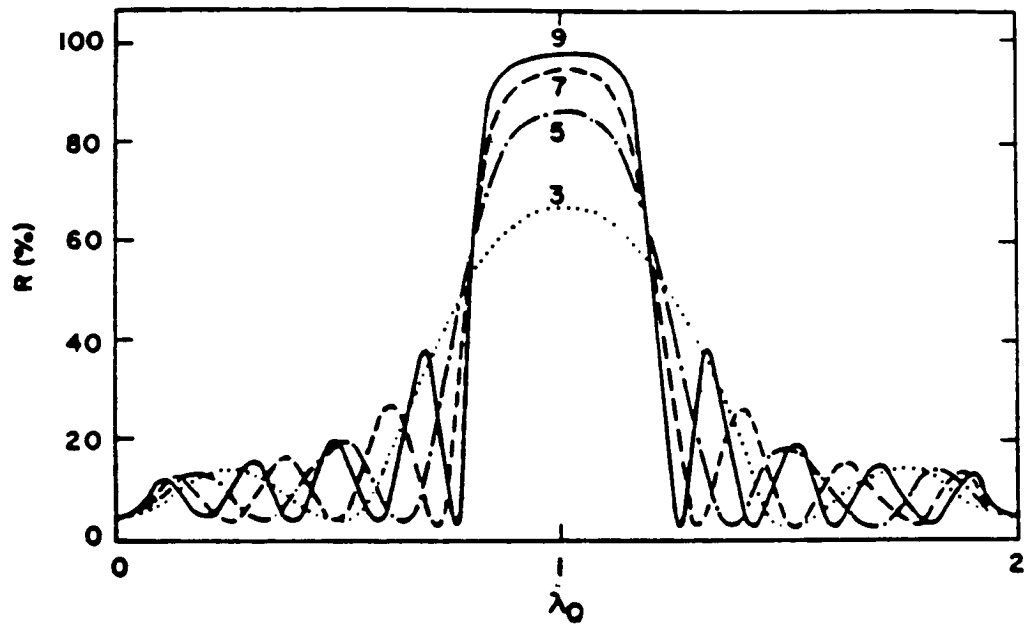

Figure 3 Normal reflectance curves of H (LH) ^{p} (p = 1,2,3,4) quarter-wave stacks of ZnS (n_H = 2.3) and MgF_2 (n_L = 1.38) on glass (n_s = 1.52)[8].

I.B. Some Examples Of Materials For Optical Thin Films.

Due to the versatility and wide application of optical coatings, the field has attracted scientists and engineers from both industry and academia. New optical coating materials and deposition methods continue to be discovered.

Magnesium fluoride has been widely used as low refractive index optical coating layer with an refractive index of n = 1.38. P. J. Martin *et al*[9] used conventional evaporation and oxygen ion-assisted deposition to make MgF_2 films on carbon substrates and obtained the refractive index of 1.37 at 550 nm. I. M. Thomas[10] successfully prepared quarterwave antireflective CaF_2 and MgF_2 coatings with near 100% transmittance on fused silica and calcium fluoride from colloidal suspensions of

relevant fluorides in methanol. The refractive index for both CaF_2 and MgF_2 was n = 1.2. Vacuum deposited MgF_2 overcoated on aluminum films can achieve high reflectance in the vacuum ultraviolet . Howard Herzig *et al*[11] deposited lithium yttrium fluoride ($LiYF_4$) and lanthanum fluoride (LaF_3) instead of magnesium fluoride and pointed out both Al + LaF3 and Al + LiF4 combinations are inferior to the Al + MgF2 from a reflectance viewpoint.

Another very important film material is zinc sulfide, n = 2.42. Q. Wu[12] used a rotating-quarterwave plate ellipsometer to determine the inhomogeneity in the refractive index of ZnS and found that when the film thickness is over 350 Å, the index remains constant.

C. G. Granqvist *et al*[13,14] prepared In_2O_3 : Sn conducting films by e-beam evaporation and inspected their properties. Granqvist pointed out that In_2O_3 : Sn films can combine high transmittance of luminous and solar radiation with low thermal emittance.

J. M. Bennett *et al*[15] used seven different methods to prepare titanium dioxide (TiO_2) films: e-beam evaporation, ion assisted deposition, ion-beam sputter deposition, activated reactive evaporation, ion or plasma plating, rf diode sputtering, and dip coating from a solution using the Schott process. They concluded that the film properties differ widely, n = 2.18 ~2.61 at λ = 550nm. SiO_2/TiO_2 multilayer coatings can achieve high-quality spectra. G. J. Exarhos *et al*[16] prepared three different SiO_2/TiO_2 multilayer devices and examined their performance. The transmittance exceeded 90% at specific wavelengths within the visible range.

Other multilayer devices have been produced. Bruce W. Smith[17] made heat mirrors with ZnS-Ag-ZnS films. The filters exhibited 87% peak transmission in the visible range, while reflecting 80% in the infrared.

I.C. Refractive Index of Silicon and Silicon Related Films

Silicon and its oxides and nitrides have a very wide range of refractive index in the visible and near infrared—6000 to 12000 Å. Reactive evaporation of silicon is quite a practical idea with the potential of easily varying n. Table 1 contains the refractive indices of some silicon and silicon related films[18].

Table 1 The refractive indices of silicon and silicon related films.

Film Materials	Wavelength Range (Å)	Refractive Index(n)
Silicon	5961—12000	3.96—3.52
a-Silicon	6199—12400	4.23—3.54
Noncrystalline Silicon Nitride	6000—12000	2.00—1.90
Silicon Dioxide(Crystalline)	5893—12000	1.54—1.53
Silicon Dioxide(Glass)	5893—11287	1.46—1.45
Silicon Monoxide(Noncrystalline)	6199—10000	1.97—1.87

The wide difference in the indices of silicon and silicon-related films allow useful optical coatings to be designed. If reactive deposition is practical, only a single source of material would be needed, potentially simplifing the deposition.

1.D. Some Samples for Silicon Related Films

Silicon nitride films were deposited onto <100> oriented 6-9 ohm-cm P-type silicon wafers by Sugawara *et al*[19]. A refractive index as low as 1.6 was reached. They made films both with silicon vapor deposition and nitrogen ion implantation. The presence of silicon nitride was confirmed with Auger Electron Spectroscopy.

Dunnett *et al* [20] prepared amorphous silicon nitride (Si_xN_{1-x}) films with r.f. glow-discharge decomposition of different ammonia-silane mixtures. The results of electrical and optical measurements varied systematically and continuously over the

entire range of gas mixtures.

Knolle and Osenbach[21] fed varying flows of nitrous oxide (N_2O) through with a constant flow of 2% silane in nitrogen, and prepared oxygen-doped, plasma-deposited silicon nitride films on 100 mm diameter, <111> , n-type silicon wafers and obtained refractive indices between 1.7 and 2.3.

Ponpon *et al*[22] adopted the rapid thermal heating method to make silicon oxide films by introducing <111> and <100> P-type silicon samples into a quartz furnace under high-purity dry oxygen atmosphere.

Eriksson *et al* and Lam made silicon oxynitride films. Eriksson[23] deposited silicon oxynitride films onto high purity silicon wafers and Corning 7059 glass plates which were precoated with opaque aluminum layers with an electron-beam evaporation system under slightly reactive condition. They determined the film composition as $SiO_{0.6}N_{0.2}$ by Rutherford backscattering spectrometry (RBS) using 2.4-MeV α-particles. Lam[24] produced silicon oxynitride films on silicon wafers with a 2-μm thermally oxidized SiO_2 buffer layer using plasma chemical vapor deposition under low temperature (200°C) conditions and produced a film with refractive index between 1.6 and 2.0.

II. THEORY

IIA. Mechanism of SiO and SiN Film Deposition

For reactive deposition of silicon oxide and silicon nitride, the starting material is silicon. A reactive gas is introduced and is ionized by energetic electrons. The electrons are emitted from a heated tungsten wire and are accelerated by a biasing voltage to ionize reactive gases. The thermionic emission of electrons can be expressed as:

$$W \text{ ----------> } W^{+n} + ne^{-1}$$

The electron interactions with the reactive gas may be represented as:

$$O_2 + e^{-1} \text{ ----------> } O_2^+ + 2e^{-1}$$
$$N_2 + e^{-1} \text{ ---------> } N_2^+ + 2e^{-1}$$

Finally the molecular ions react with the silicon in the growing film to produce SiOx or SiNx. The oxygen reaction might be:

$$Si + O_2^+ \text{ ----------> } SiO_2^+$$

This process is similar to reactive ion-planting deposition[25]. In ion planting, however, ions of the evaporated species are accelerated to the substrate where they may cause secondary sputtering of the growing film. In this thesis, only reactions are considered.

In the method of this thesis, film composition will vary with the amount of reactive gas. When the reactive gas pressure is high, I expect the film to contain more low-index silicon oxide or silicon nitride and have less high-index silicon. This results in a low refractive index for the film.

IIB. Optics Of Thin Film Coatings[8]

Consider electromagnetic radiation incident on a boundary separating two media of indices of refraction n_0 and n_1 with an incident angle θ, as shown in Figure 5. Some of the incident radiation will be reflected back into the incident medium, while some will pass into the second medium.

The complex optical admittance, N, for one specific material can be expressed in terms of the refractive index n and the extinction coefficient k, as:

$$N = n - ik.$$

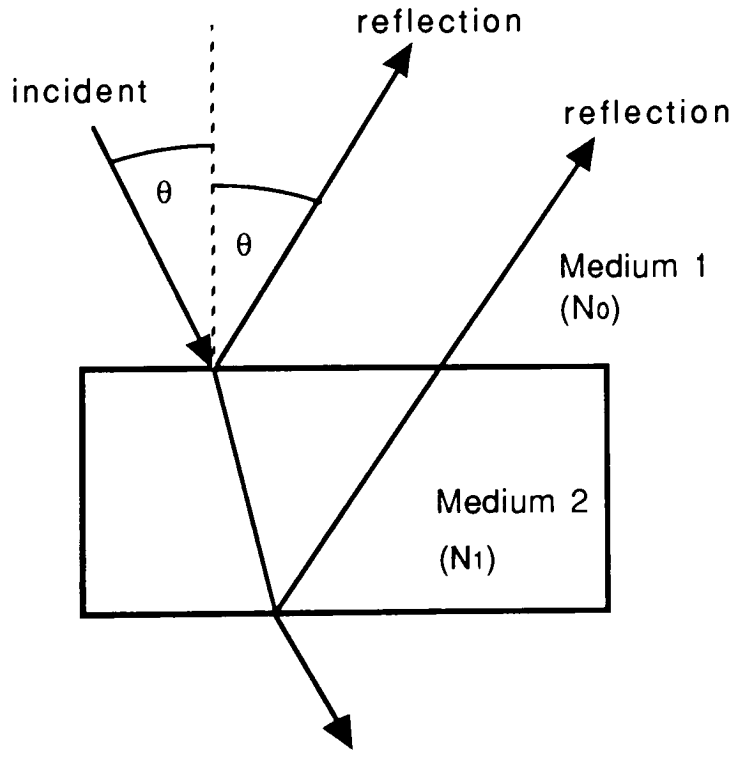

Figure 4 Reflection from a thin film. If reflectance is small, only the first two reflected beams are considered; if reflectance is larger, the Fresnel multiple beam method must be applied[2].

It is convenient to define the complex effective optical admittance, η, for a medium. This combines the refractive index and the incident angle and is defined differently for the two polarization directions:

For TE waves, $\eta = N \cos\theta$

For TM waves, $\eta = N / \cos\theta$

For a single layer of Figure 4, the reflectance R can be calculated as:

$$R = \left| \frac{\eta_0 - \eta_1}{\eta_0 + \eta_1} \right|^2 \qquad (1)$$

where η_0 and η_1 are the effective optical admittances for media 1 and 2.

Next consider a system composed of i (i = 1 to L) layers deposited on a substrate of admittance N_s, with the outermost layer was defined as i =1. Light of vacuum wavelength λ is incident and θ_i is the angle of refraction at the i^{th} layer. Each layer has a characteristic admittance of N_i and a thickness t_i. The admittance of the incident medium is N_0. The reflectance is then determined by the complex effective optical admittance of the assembly, Y, as:

$$R = \left| \frac{\eta_0 - Y}{\eta_0 + Y} \right|^2 \qquad (2)$$

Herpin developed a matrix method to determine Y. The first step is to calculate the characteristic matrix of the system. The characteristic matrix of a system is the product of matrices for the individual layers. The i^{th} layer has an effective phase thickness, δ_i, defined as

$$\delta_i = (2\pi / \lambda) (N_i t_i \cos\theta_i) \qquad (3)$$

Starting from the substrate with effective optical admittance η_s, the effect at the surface is given by:

$$\begin{bmatrix} B \\ C \end{bmatrix} = \prod_{i=1}^{L} \begin{bmatrix} \cos\delta_i & \iota \sin\delta_i / \eta_i \\ \iota \eta_i \sin\delta_i & \cos\delta_i \end{bmatrix} \begin{bmatrix} 1 \\ \eta_s \end{bmatrix} \tag{4}$$

Finally, Y is defined as:

$$Y = C / B \tag{5}$$

In a non-absorbing single film device, the characteristic matrix can be calculated as following:

$$\begin{bmatrix} B \\ C \end{bmatrix} = \begin{bmatrix} \cos\delta_1 & \iota \sin\delta_1 / \eta_1 \\ \iota \eta_1 \sin\delta_1 & \cos\delta_1 \end{bmatrix} \begin{bmatrix} 1 \\ \eta_s \end{bmatrix}$$

$$= \begin{bmatrix} \cos\delta_1 + \iota (\eta_s/\eta_1) \sin\delta_1 \\ \eta_s \cos\delta_1 + \iota \eta_1 \sin\delta_1 \end{bmatrix}$$

From Equation (5)

$$Y = \frac{C}{B} = \frac{\eta_s \cos\delta_1 + \iota \eta_1 \sin\delta_1}{\cos\delta_1 + \iota (\eta_s/\eta_1) \sin\delta_1} \tag{6}$$

Substituting Equation (6) into Equation (2)

$$R = |(\eta_0 - Y) / (\eta_0 + Y)|^2$$

$$= [\eta_0^2 - \eta_0 (Y + Y^*) + Y^* Y] / [\eta_0^2 + \eta_0 (Y + Y^*) + Y^* Y]$$

Since $$Y + Y^* = \frac{2 \eta_1^2 \eta_s}{\eta_1^2 \cos^2\delta_1} + \eta_s^2 \sin^2\delta_1$$

and $$Y Y^* = \frac{\eta_1^4 \sin^2\delta_1 + \eta_1^2 \eta_s^2 \cos^2\delta_i}{\eta_1^2 \cos^2\delta_1 + \eta_s^2 \sin^2\delta_1}$$

$$R = \frac{(\eta_0 - \eta_s)^2 \cos^2\delta_1 + [(\eta_0 \eta_s / \eta_1) - \eta_1]^2 \sin^2 \delta_1}{(\eta_0 + \eta_s)^2 \cos^2 \delta_1 + [(\eta_0 \eta_s / \eta_1) + \eta_1]^2 \sin^2 \delta_1}$$

If a single layer of a quarter-wavelength thickness ($nt = \lambda /4$) were deposited onto the substrate at normal incidence, $\theta = 0$, then :

$$\delta_i = (2\pi / \lambda)(\lambda / 4) \cos 0) = \pi /2$$

and

$$R = 0 + [(\eta_0\eta_s / \eta_1) - \eta_1]^2 / [(\eta_0\eta_s / \eta_1) + \eta_1]^2$$

$$= (n_0n_s - n_1^2 / n_0n_s + n_1^2)^2$$

This means that when $n_1^2 = n_0n_s$, the reflectance will be reduced to zero.

A more complicated device is a double layer, quarter- wave coating with the outer layer having a larger refractive index (n_1) than the inner one (n_2), and light incident from air. The equivalent optical admittance (Y) of this system can be calculated as:

$$\begin{bmatrix} B \\ C \end{bmatrix} = \begin{bmatrix} \cos \delta_1 & \iota \sin \delta_1 / \eta_1 \\ \iota \eta_1 \sin \delta_1 & \cos \delta_1 \end{bmatrix} \begin{bmatrix} \cos \delta_2 & \iota \sin \delta_2 / \eta_2 \\ \iota \eta_2 \sin \delta_2 & \cos \delta_2 \end{bmatrix} \begin{bmatrix} 1 \\ \eta_s \end{bmatrix}$$

$$= \begin{bmatrix} \cos \delta_1 \cos\delta_2 - (\eta_2/\eta_1) \sin \delta_1 \sin \delta_2 + \iota \eta_s (\sin \delta_2 \cos \delta_1 / \eta_2 + \sin \delta_1 \cos \delta_2 / \eta_1) \\ \iota \eta_1 \sin \delta_1 \cos \delta_2 + \iota \eta_2 \sin \delta_2 \cos \delta_1 - \eta_s((\eta_1/\eta_2) \sin \delta_1 \sin \delta_2 - \cos \delta_1 \cos \delta_2) \end{bmatrix} \quad (8)$$

At normal incidence, the phase thicknesses are $\delta_1 = \delta_2 = \pi /2$ and Equation (8) can be simplified.

$$\begin{bmatrix} B \\ C \end{bmatrix} = \begin{bmatrix} \frac{-\eta_2}{\eta_1} \\ \frac{-\eta_s \eta_1}{\eta_2} \end{bmatrix}$$

$$Y = C/B = \eta_1^2 \eta_s / \eta_2^2 \qquad (9)$$

Substituting Equation (9) into Equation (2)

$$R = |(\eta_0 - Y)/(\eta_0 + Y)|^2 = [\{1 - (\eta_1^2 \eta_s / \eta_2^2)\} / \{1 - (\eta_1^2 \eta_s / \eta_2^2)\}]^2$$

$$= [\{1 - (n_1/n_2)^2 n_s\} / \{1 + (n_1/n_2)^2 n_s\}]^2$$

Since $n_1 > n_2$, $n_1/n_2 > 1$ and $(n_1/n_2)^2 n_s > 1$. So

$$R = \left[1 - \frac{2}{1 + (n_1/n_2)^2 n_s}\right]^2$$

As n_1/n_2 increases, R increases. If n_1/n_2 is large enough, a high reflection coating can be achieved.

For example, consider a glass slide designed to have high reflectance at 2 μm. The required thicknesses of one quarter-wave of silicon monoxide ($n_2 \sim 2.0$) and one quarter-wave of silicon ($n_1 \sim 4.0$) are 2500 Å for the SiO and 1250 Å for the Si and the reflectance is

$$R = \{1 - 2/[(2^2 * 1.5) + 1]\}^2 = 0.51 = 51\%$$

III. Experiment

IIIA. Substrate And Sample Preparation

In this thesis, both 25mm x 75mm plain glass slides and silicon wafers were used as substrates. The glass slides were pre-cleaned with the following procedure. The slides were scrubbed with Alconox and water, and rinsed thoroughly with hot tap water. They were immersed in a Branson 2200 ultrasonic cleaner in distilled water with heat for a half hour. After removal, they were rinsed with methanol and air dried. After deposition, the glass slides were taken to the spectrophotometer to obtain the infrared spectra. Films were deposited on one side of $2^1/_4$ inch diameter silicon wafers. No cleaning procedures were used for the silicon wafers. The silicon samples were originally intended for ellipsometric measurements.

IIIB. E-Beam Coater Basics

Silicon was evaporated from a Temescal Model SFIH-270-2 single hearth electron-beam source. A standard diffusion pumped system pumped the vacuum chamber to a base pressure of around 5×10^{-6} Torr. Figure 5 is a sketch of the coater. Substrates were heated to 150°C with a quartz IR lamp under the control of an Omega Temperature Controller. A temperature detector, put on the back of the glass slides, recorded the highest substrate temperature. After opening the chamber, the substrate temperature could be read and compared with the set point of the controller.

Normally when the Omega Temperature Controller was set at 200°C, the substrate was heated up to 150°C. The substrate holder could be rotated, and four sample positions were available. Substrate alignment was confirmed with either indicator marks on the rotary gears or by observation from the chamber window. A shutter was placed immediately above the source. The deposition rates and thickness were measured with an Inficon quartz crystal monitor. Various deposition rates could be

obtained by varying the accelerating voltage and current of the e-beam. In this experiment, accelerating voltage was between 5 and 6 kV while e-beam current was between 0.2 and 0.4 A. Deposition rates varied with evaporation conditions as will be described later. Oxygen or nitrogen gas was fed into the chamber through a Tylan mass flow controller. Pressures were measured with an ionization gauge.

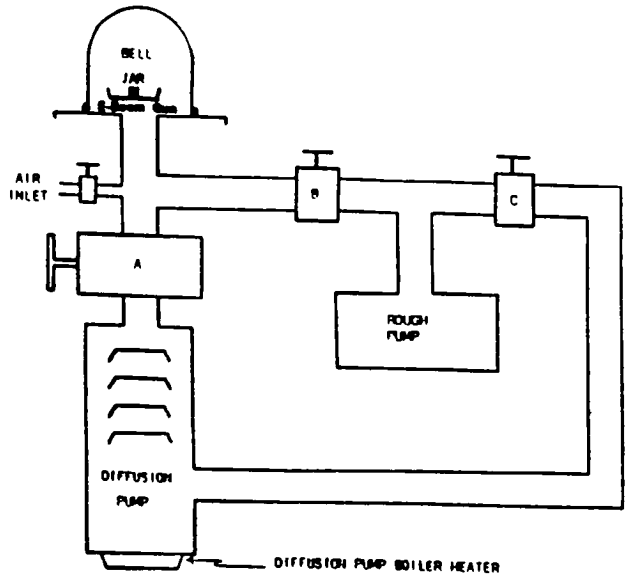

Figure 5 Sketch of the e-beam coater.

IIIC. Silicon Source Material

The source was solid silicon (99.99% pure) which was held in the anode of the e-gun. Before deposition, the filament power was turned on and an e-beam current between 0.2 and 0.4 A was focused onto the anode by electromagnetic coils and permanent magnets. This action kept the e-beam concentrated on the surface of the evaporant and a pool of molten evaporant was continually formed. The point of impact of the electrons was moved around the surface of the silicon in order to maintain a high evaporation rate. Once the source was well melted, the filament power and e-beam current was adjusted to reach a specific deposition rate. After the deposition, the shutter was closed, and both the filament power and e-beam current were shut off

at once to avoid excess silicon deposition.

The deposition rate and thickness were measured with an Inficon rate deposition monitor which was located substantially above the samples. In addition, the monitor crystal had an aperture in front of it (part of the rotational feedthrough). These two system constraints meant that the tooling factor was quite large. At high pressures, the evaporated silicon had a short mean free path, and this made it more difficult for the monitor to accurately gauge the true deposition rate. This led to large uncertainties in the tooling factors. The thickness of all deposits were measured on the Dektak Surface Profilometer, so that accurate measures of thickness and rate were obtained after deposition.

IIID. Gas Input

Nitrogen and oxygen gases were introduced into the chamber through a Tylan mass flow controller. Nitrogen gas was fed in to reach pressures between 3.0×10^{-5} Torr and 2.0×10^{-4} Torr in order to attempt activated reactive evaporation of silicon nitride. Oxygen was introduced into the chamber to reach pressures between 2.0×10^{-5} and 2.0×10^{-4} Torr in order to form silicon oxides. During silicon nitride deposition, the chamber pressures remained fixed, while for silicon oxide deposition, chamber pressures decreased abruptly once the silicon was melted and began to evaporate. The drop in pressure indicated some oxygen must be reacting with the freshly deposited film, and this was initial evidence of reactive evaporation.

IIIE. Tungsten Wire And Biasing

In order to enhance the process of reactive deposition, a simple ionizer was put into the chamber as shown in Figure 6a. The details of the ionizer are shown in Figure 6b. The ionizer was composed of a tungsten wire which was heated by a Variac to thermionically emit electrons. The electron current was controlled at around 160mA by

adjusting the Variac. This usually required 70 V of AC current. The wire was biased negatively with respect to the chamber ground by a 0 to 500 V biasing voltage. The electrons were accelerated to ground consisting of the gas feed line and the chamber. Silicon vapor contaminated the hot filament, and it was changed frequently so that the wire would not burn out during deposition and ruin the experimental run.

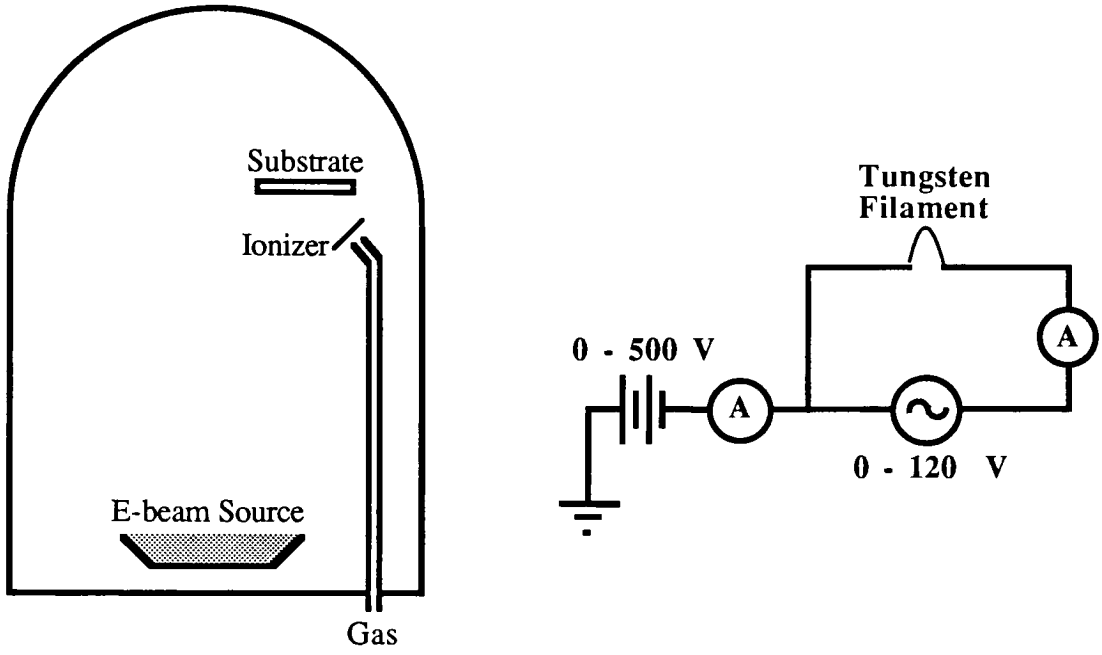

(a) (b)

Figure 6. Schematic diagram of electron beam evaporation system with ionizer. The amount of the electrons released from the hot tungsten wire was large enough to provide substantial ionization of the gas.
(a) Overall schematic of the coater.
(b) Electrical schematic of the ionizer.

IIIF. Measuring the Refractive Index with a Spectrophotometer

A Cary Model 14 Spectrophotometer was used to obtain infrared (6000 ~ 26000Å) transmittance spectra of the deposited films at normal incidence. The index of refraction, n_f, of a film can be determined from the results as follows. Light reflected

from the air-film surface and the film-substrate surface must have a phase difference (ø) as shown in Figure 8. The ϕ_p are appropriate for p-polarized light, and their difference is π. For s-polarized light the phase shifts are opposite that shown, but the difference is still π.

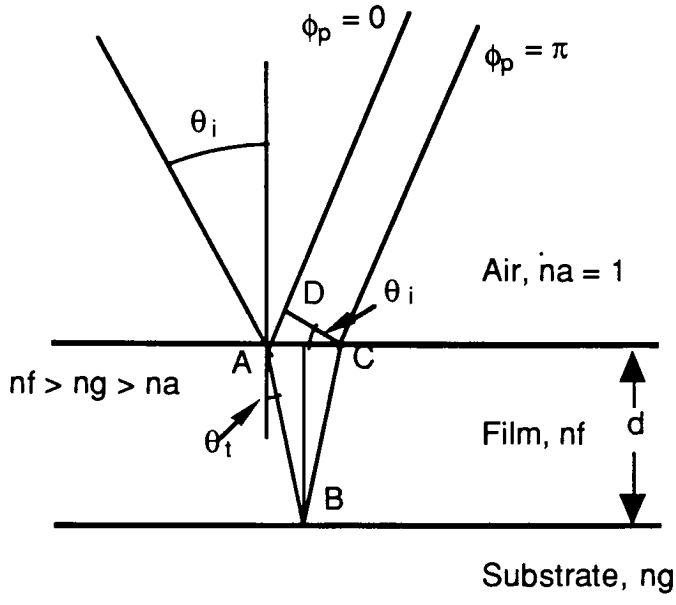

Figure 7.[2] Phase difference between reflected beams from two sides of a single layer film. The ϕ represent phase change upon reflection.

The optical path length difference, Δ , can be expressed as[2]:

$$\Delta = n_f \ (AB+BC) - n_a \ AD$$

$$= 2 \ n_f d \cos \theta_t$$

The total phase difference from both optical path difference and phase shift arising from reflection is

$$ø = (2 \ n_f d \cos\theta_t / \lambda) * 2\pi + \pi$$

With normally incident light, $\theta_t = 0$,

$$2\, n_f\, d \cos \theta_t = 2\, n_f\, d$$

so constructive (maximum reflectance) and destructive (minimum reflectance) interference should occur for $\phi = 2\pi N$ and $\phi = 2\pi (N + 1/2)$ respectively. The condition for an extremum in the reflectance (or transmittance) versus wavelength curve can be written

$$2 n_f d = M \lambda$$

where $M = N + 1/2$ for a reflectance maximum or transmittance minimum transmission and $M = N$ for a reflectance minimum or transmittance maximum.

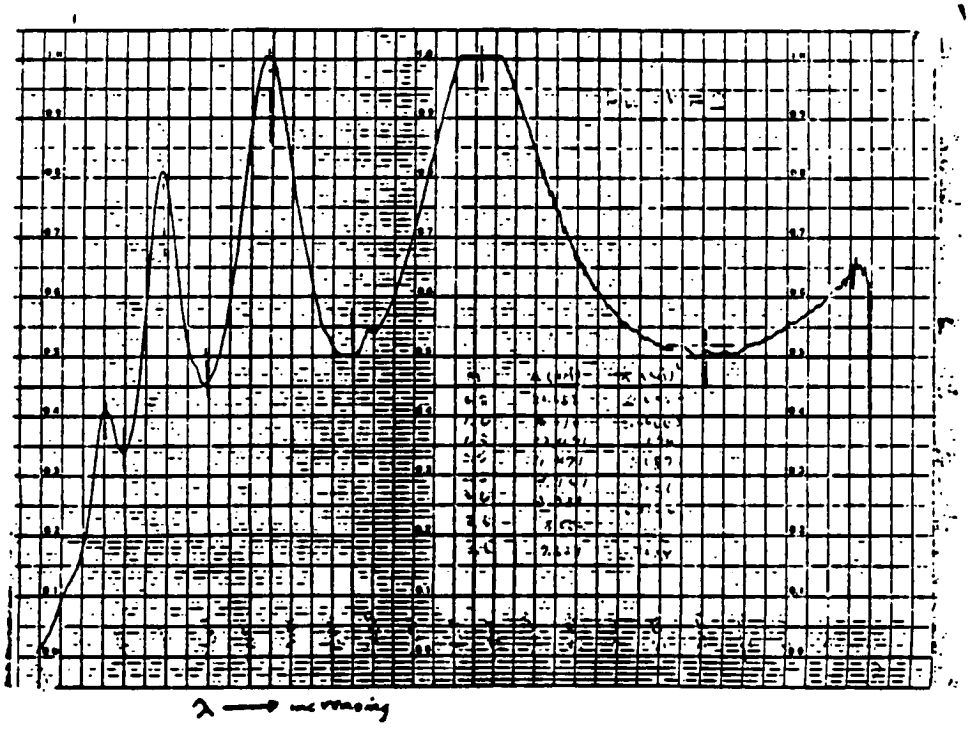

Figure 8 A typical spectrophotometer trace of transmittance versus wavelength.

For a fixed index, n_f, and thickness, d, measured maxima and minima occur at wavelengths λ_i corresponding to M_i satisfying

$$M_i = (2\, n_f\, d) * (1/\lambda_i)$$

A graph of M_i versus $1/\lambda_i$ should be linear with a slope of $(2\, n_f\, d)$. The refractive index n_f can be found by dividing the slope by 2d. A Dektak Surface Profilometer was used to determine the film thickness, d. Figure 8 and Figure 9 show a typical transmittance spectrum and an M versus $1/\lambda$ graph.

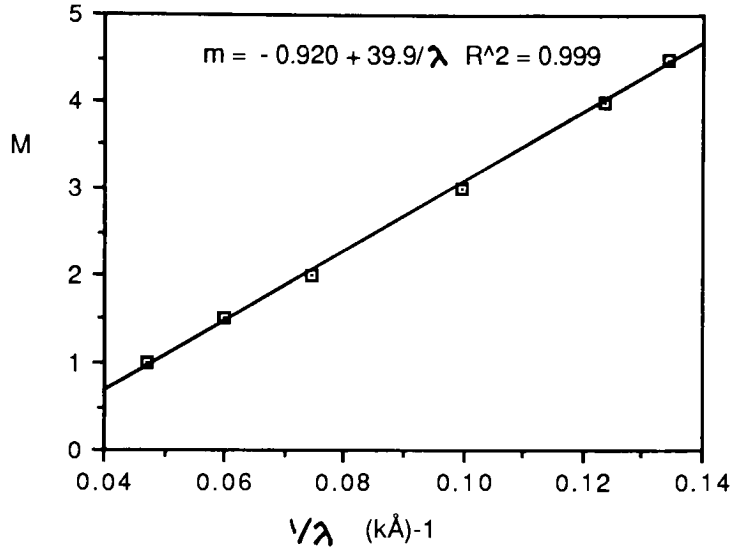

Figure 9 The M versus $1/\lambda$ graph corresponding to Figure 8. R is the correlation coefficient.

IIIG. Ellipsometry

An ellipsometer was used to measure the refractive indices of films deposited on silicon wafers. A beam with the wavelength of 550 nm was reflected from the sample. A dedicated computer calculated the value of n from this measurement. The software assumed that the film was transparent which is not necessarily the case here. Because of this, and because of the fixed wavelength, the results were not informative, and are not included in this thesis. Use of the ellipsometer was provided by Consolidated Vacuum Corporation.

IIIH. Thermal Stability

In order to inspect the thermal stability of films, samples were put into a Model 55342-4 Lindberg Furnace with a Eurotherm Controller. The furnace is 36 inches in length, 6 inches in diameter, and has a quartz reaction tube. Samples were placed in the center of the tube. Samples were heated in air to 500°C from room temperature, left there for an hour, then cooled down to room temperature slowly. This temperature was arbitrarily chosen to be well above the substrate temperature during deposition. After the heat treatment, the refractive indices of the samples were remeasured by the spectrophotometer. The new values were compared with the old ones to see if the films had been further oxidized. Two samples, one each of high and low refractive index, were annealed.

IIII. Fourier Transform Infrared Spectroscopy

Fourier Transform Infrared Spectroscopy (FTIR) was done on samples in order to identify the composition of the films. Silicon and silicon oxide films were deposited onto sodium chloride FTIR cells and were measured on a Perkin Elmer Model 1700 FTIR Spectrometer. One beam was focused on the sample and scanned over the middle infrared region (4000~400 cm^{-1}). The absorption bands provide the information about the chemicxal composition of the film. Three samples were measured, a pure silicon film, silicon oxide prepared at 2.0 x 10^{-4} Torr of oxygen and 5 Å/sec, and silicon oxide prepared at 2.0 x 10^{-4} Torr of oxygen and 11 Å/sec. The results were compared to determine the existence silicon oxide bonds, and to find out if different deposition rates and chamber pressures affected the composition of films.

IIIJ. Visual Inspection

Since the film properties depend strongly on deposition conditions, the appearances of samples vary. Slides coated with pure silicon looked grey and dark. Slides with silicon evaporated in nitrogen with no electrical discharge were the same as the pure silicon films. Those slides produced by evaporating silicon in nitrogen with a hot filament with or without a bias voltage look dark brown.

In the silicon oxide system, factors were changed over a wide range, so the slides varied in appearance. Some samples looked very dark. They were similar to the pure silicon samples. In other cases, the samples were very transparent. Generally speaking, films with a real refractive index, and thus no absorption, such as silicon nitrides and silicon oxides, should be transparent. This is a rough way to tell the existence of silicon oxides, however, other more precise method, such as FTIR, must be employed to inspect the film composition. Visual results will be described later.

IV. Results

IVA. Statistical Analysis of the Results

Since there are four variables to be controlled—chamber pressure, substrate temperature, deposition rate and biasing voltage, a statistical approach was adopted based on analysis of variance (ANOVA). Here two values for each parameter were chosen and all possible combinations of these parameters were tested. Thus for four parameters, $2^4 = 16$ experiments must be done [27].

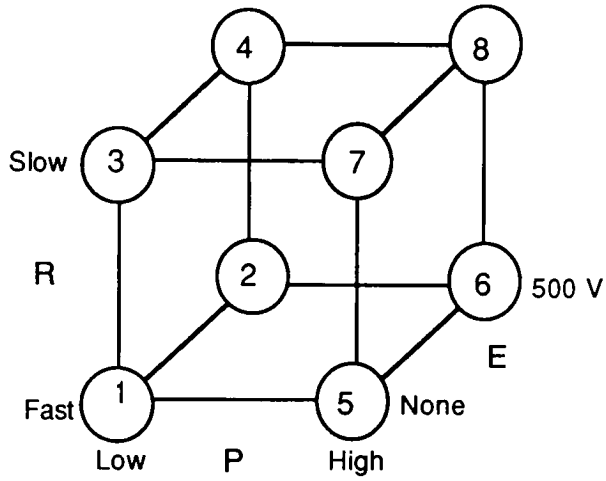

Figure 10. Geometrical representation of a 2^3 full factorial experiment in rate, R, pressure, P, and electric biasing, E.

The idea can be understood more easily for a 2^3 experiment in three variables. If we plot the variables along three orthogonal axes, the eight possible combinations of variables produce a cube, as shown in Figure 10. To assess the effect of one variable, such as pressure, P, we can average the left square of measurements, 1, 2, 3, and 4, and compare with the average of the right square of measurements, 5, 6, 7, and 8. Interactions between variables can be determined by looking at other planes in the cube. For example, the interaction of rate, R, and pressure, P, can be assessed by comparing the average of 3 and 4 with the average of 5 and 6. The full analytical

technique is derived by Box, Hunter, and Hunter[27], some details of which are given in the appendices. A measure of the standard error for a design like this can be obtained by repeating some of the measurements.

IVB. Silicon Films

Pure silicon films deposited on glass substrates all looked about the same in color—dark grey. The refractive indices of pure silicon films were measured with a spectrophotometer and the film thickness was obtained by Dektek Surface Profilimeter. Figure 12 is a typical transmittance spectrum of a pure silicon sample deposited under 7 kV, 0.3 A condition with the substrate heated to 150°C.

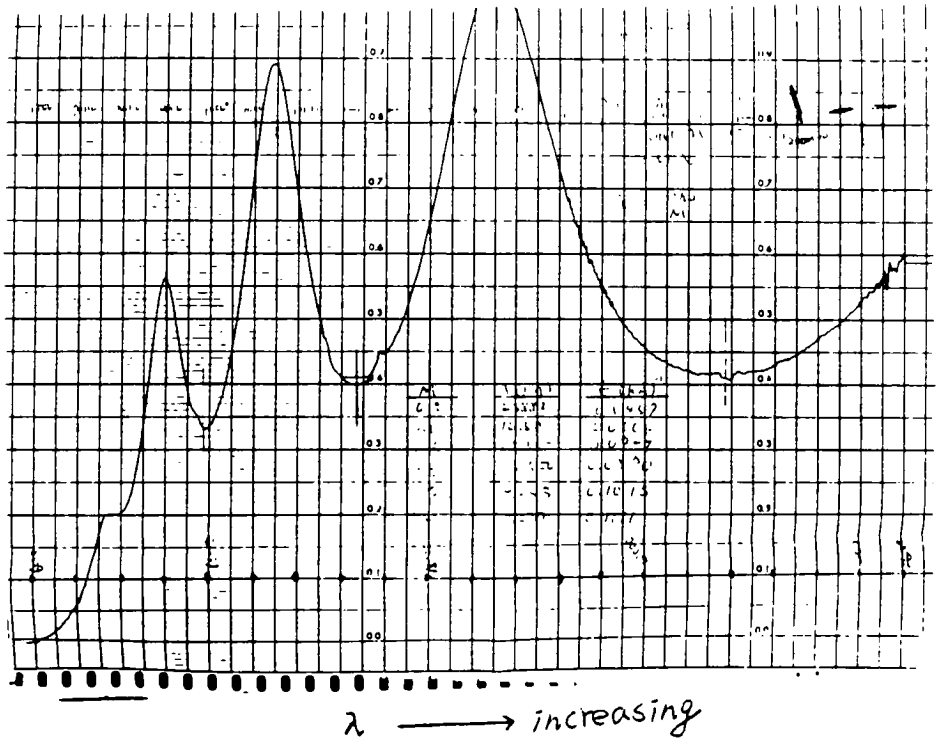

Figure 11. Spectrophotometer spectrum of a pure silicon sample.

Wavelengths for maxima and minima of the curve in Figure 11 are shown in Table 2.

Table 2 Minima and maxima points and their occuring wavelengths from Figure 11.

M	(kÅ)	$1/\lambda$ (KÅ)$^{-1}$
1	21.88	0.0457
1.5	16.50	0.0606
2	13.35	0.0749
2.5	11.50	0.0870
3	9.85	0.1015
3.5	9.00	0.1111

With the above data, one can make a M versus $1/\lambda$ graph, as shown in Figure 12.

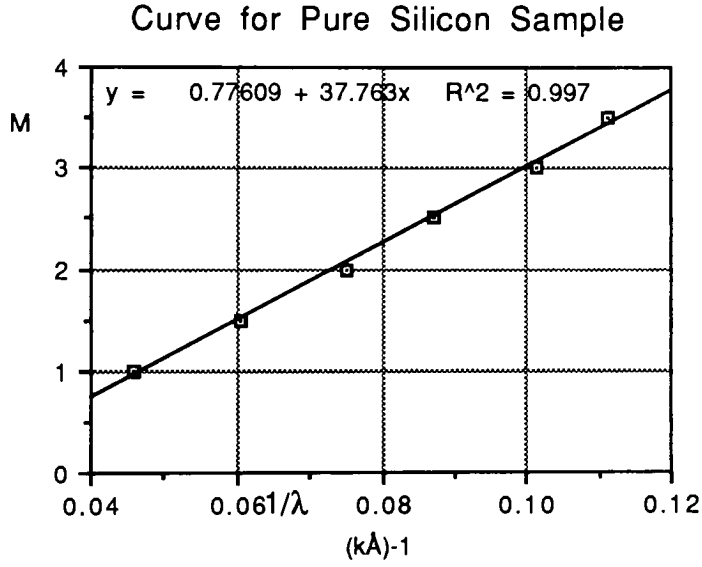

Figure 12. The M versus $1/\lambda$ graph of a pure silicon sample.

This film had a thickness of 4.52 kÅ, so the film refractive index is:

$$n_f = \text{slope} / 2d = 4.18$$

Results obtained from the spectrophotometer for several silicon films are listed in Table 3.

The average silicon film refractive index obtained from the spectrophotometer is 4.31± 0.12. Even though all of the films were produced under different conditions, the refractive indices are quite close.

For a fifth sample, pure silicon was deposited onto a glass slide and a sodium chloride IR cell. Film composition was determined with FTIR. Figure 13 is the infrared spectrum of silicon film and Table 4 is the composition of silicon film. Since the Si-O bond doesn't exist, there is no silicon oxide within the film. The C-H bond will be discussed later.

Table 3 Refractive indices of silicon films obtained from the spectrophotometer.

Sample	e-Beam	Rate Å/sec	Substrate Temp. °C	Index, n
A June 12	7 kV, 0.3A	24.5	120	4.18
B June 13	7 kV, 0.3A	23.5	120	4.39
C May 31	7 kV, 0.3A	14.97	120	4.25
D May 8	5.5 kV, xA	19.19	150	4.42

In sample D, the e-beam current was unknown because the current gauge was out of order.

Table 4 The composition of a silicon film from the FTIR spectrum in Figure 13.

Name of Bond	Wavenumber(cm^{-1})	Exist
Aliphatic C-H Bond, Stretch	2900 ~ 3000	No
Si-O	~ 1000	No

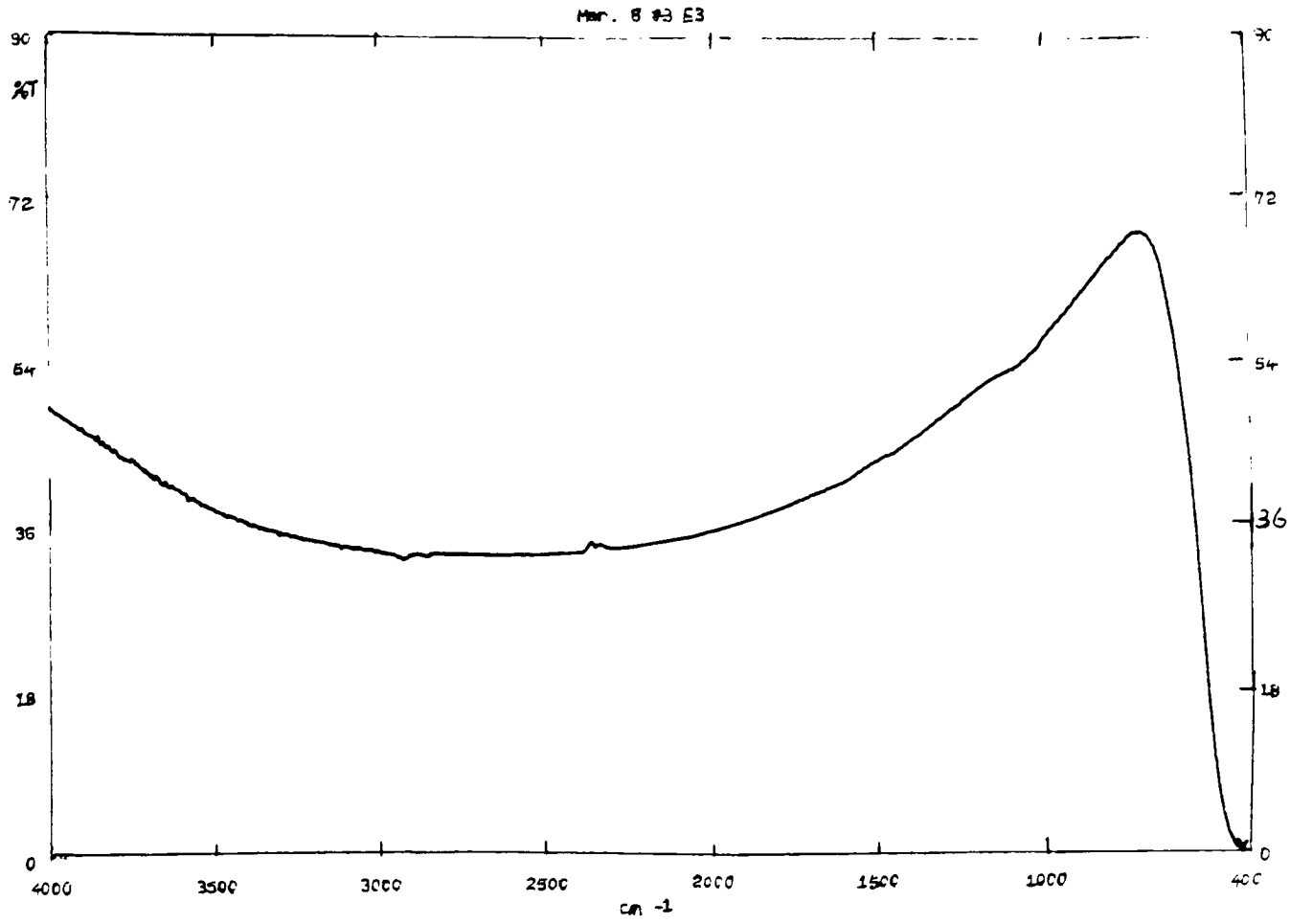

Figure 13. The FTIR spectrum of a silicon film.

IVC. Silicon Nitride Films

Regardless of the ionization scheme or deposition conditions, the silicon film deposited in a nitrogen atmosphere always looked dark grey or dark brown, similiar to silicon films. The refractive index was always high (usually $n > 4.0$), indicating no SiN formation by reactive evaporation.

IVD. Silicon Oxide Films

In the silicon oxide system, I first assumed there were four important factors which affect the film refractive index—substrate temperature, deposition rate, chamber pressure and biasing for the tungsten wire. Several sets of experiments were designed to follow up this assumption and to determine:

(1) which factors or combinations of factors are important.

(2) how the factors affect film properties.

(3) what specific conditions achieve specific films

(4) what range of refractive indices can be produced.

Factorial designed experiments were used to examine the factors. Two values for each variable were used. The results were statistically analyzed to calculate the main and interaction effects. These effects were then compared with the population standard deviation. If the values of some effects were larger than the standard deviation, the effect was deemed to be significant.

1. First Designed Factorial Experiment

In this experiment, films were deposited onto twenty-six pairs of glass slides under sixteen different conditions with randomly selected conditions. Tables 5 and 6 list the conditions and replicate numbers.

Table 5 The variables and their meanings for first designed factorial experiment.

Code	Temperature	Chamber Pressure (Torr)	Electrical Bias Voltage	Deposition Rate* Å/sec
–	Room Temp.	2.0×10^{-4}	None	18
+	150°C	2.0×10^{-5}	500 V	5

* Tooling factors varied from run to run. Deposition rates were controlled to be close to the desired value but actual rates were determined from thickness and time.

Table 6 The sixteen conditions for the first experiment.

Sample	Temperature	Pressure	Rate	Biasing	Repeats
1	Low	High	Fast	Low	1
2	Low	High	Fast	High	2
3	Low	High	Slow	Low	2
4	Low	High	Slow	High	1
5	Low	Low	Fast	Low	3
6	Low	Low	Fast	High	1
7	Low	Low	Slow	Low	1
8	Low	Low	Slow	High	1
9	High	High	Fast	Low	1
10	High	High	Fast	High	2
11	High	High	Slow	Low	1
12	High	High	Slow	High	5
13	High	Low	Fast	Low	2
14	High	Low	Fast	High	1
15	High	Low	Slow	Low	1
16	High	Low	Slow	High	1

Table 7 The results of the first experiment.

Sample	Deposition Rate Å/sec	Refractive Index (n)	Average n
1	19.27	3.15	3.15
2	8.35, ~8.0	3.01, 2.36	2.68
3	5.80, 4.18	2.43, 3.29	2.86
4	5.07	2.40	-
5	16.63,16.92	2.10, 2.15	2.13
6	7.48	3.25	3.25
7	4.35	2.37	2.37
8	4.6	3.47	3.47
9	13.3	1.90	1.90
10	10.24, 9.96	2.39, 2.39	2.39
11	6.42	2.76	2.76
12	7.02, 7.66, 6.74, 6.63,5.88	2.38,1.84, 2.09, 2.01, 2.22	2.11 ± 0.20
13	14.08,11.03	2.12, 3.84	2.98
14	12.67	2.24	2.24
15	4.17	3.34	3.34
16	5.02	1.83	1.83

The refractive indices of slides are in Table 7. Several conditions were repeated, especially the condition #12—high temperature, high pressure, slow deposition rate, and high bias voltage which was repeated five times since it was expected to produce low refractive index films. The standard deviation of the five samples in run #12 was 0.20. A full analysis of variance gives an estimate for the standard error of the index of 0.326.

The sixteen (2^4) conditions of first set of experiment can be displayed geometrically in two blocks as in Figure 14. For the four variables, two levels of temperature (T), chamber pressure (P), bias voltage (E), and deposition rate (R) were employed to investigate the main and interaction effects. For convenience, – signs indicate high pressure, fast deposition rate, room temperature, or no biasing; while + signs indicate low pressure, slow deposition rate, high temperature, or high bias voltage.

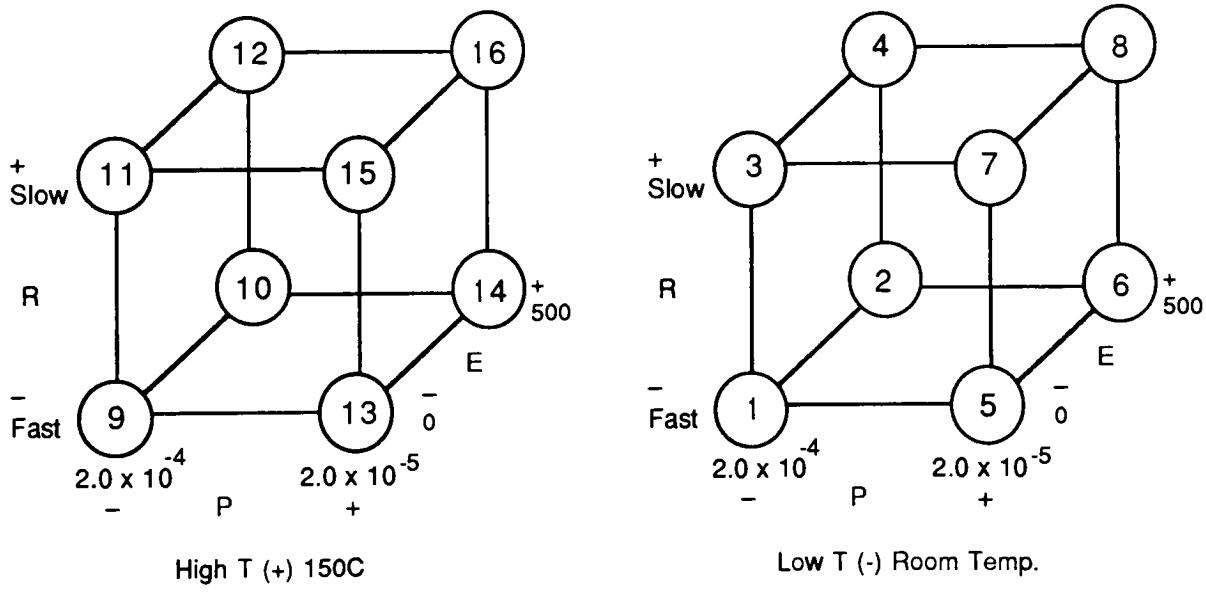

Figure 14. First experiment with conditions displayed geometrically

The effect of each factor can be calculated as shown in Appendix 1. Appendix 2 is a summary of Yates algorithm for quickly determining the effects.

Table 8 Statistics on the effects for the first experiment with 2^4 conditions[27].

N	E	R	P	T	Index	Dof	Effects	
1	-	-	-	-	3.15	16	Ave	2.616
2	+	-	-	-	2.68	8	E	-0.140
3	-	+	-	-	2.86	8	R	0.053
4	+	+	-	-	2.40	8	ER	-0.240
5	-	-	+	-	2.13	8	P	0.170
6	+	-	+	-	3.25	8	EP	0.133
7	-	+	+	-	2.37	8	RP	0.050
8	+	+	+	-	3.47	8	ERP	0.043
9	-	-	-	+	1.90	8	T	**-0.345**
10	+	-	-	+	2.39	8	ET	**-0.463**
11	-	+	-	+	2.76	8	RT	0.080
12	+	+	-	+	2.11	8	ERT	-0.238
13	-	-	+	+	2.98	8	PT	0.138
14	+	-	+	+	2.24	8	EPT	**-0.655**
15	-	+	+	+	3.34	8	RPT	-0.208
16	+	+	+	+	1.83	8	ERPT	0.050

-	0	Fast rate	High pressure	Cold	Estimate of s = 0.326
+	500	Slow rate	Low pressure	Hot	

Those effects in Table 8 which exceed the estimate of s = 0.326 are definitely significant. Those with effects which approach s may or may not be significant. Using this criterion, I found that:

(1) Temperature is the strongest main effect, pressure and electrical discharge have little effect, while rate has nearly no effect. The refractive indices obtained for depositions at low substrate temperature are all above 2.00 and the highest one is 3.47. For the high substrate temperature ones, the lowest one is 1.83 and the range of refractive indices seems larger. So I believe the high temperature will more likely provide the desired (very low n) film.

(2) Of the two way interactions, ET is significant while ER approaches significance. I don't expect ER to be large since neither E nor R effects are considered important.

(3) One three way interaction, EPT appears significant even though neither E nor P are significant. Large values for ERT and RPT add to the confusion, suggesting the need for further experiments.

Since many of the lowest values of n occur for high substrate temperature I reanalyzed a subset of high temperature conditions. Here the analysis was reduced to a 2^3 factorial design since the substrate temperature for each condition is the same. The results are in Table 9.

Table 9 Statistics on the effects of a high temperature subset of the first experiment.

–	No Bias	Fast Rate	High Pressure
+	500 V	Slow Rate	Low Pressure

N	E	R	P	n	DOF	Effects	
9	-	-	-	1.90	8	Ave	2.444
10	+	-	-	2.39	4	E	**-0.603**
11	-	+	-	2.76	4	R	0.133
12	+	+	-	2.11	4	ER	**-0.478**
13	-	-	+	2.98	4	P	**0.308**
14	+	-	+	2.24	4	EP	**-0.522**
15	-	+	+	3.34	4	RP	-0.158
16	+	+	+	1.83	4	ERP	0.093

From Table 9, one can conclude that for elevated substrate temperature:

(1) Presence of electrical bias is significant, as is the pressure, while deposition rate has little effect.

(2) Two way interactions ER and EP are significant in part because of the strong effect of E. The interactions can be examined in Figures 15 and 16 which are projections of the design cube in E, R, and P onto a two dimensional plane.

In Figure 15 we see that both the best (low n—1.8, 2.1) and the worst (high

n—3.3, 2.8) conditions occur at low rate. This is surprising because rate was calculated to have nearly no effect in Table 8. For low rates, when electrical biasing increased, n always decreased (2.8→ 2,1, 3.3 → 1.8). The results are less consistant at high rates, indicating an interaction between the variables.

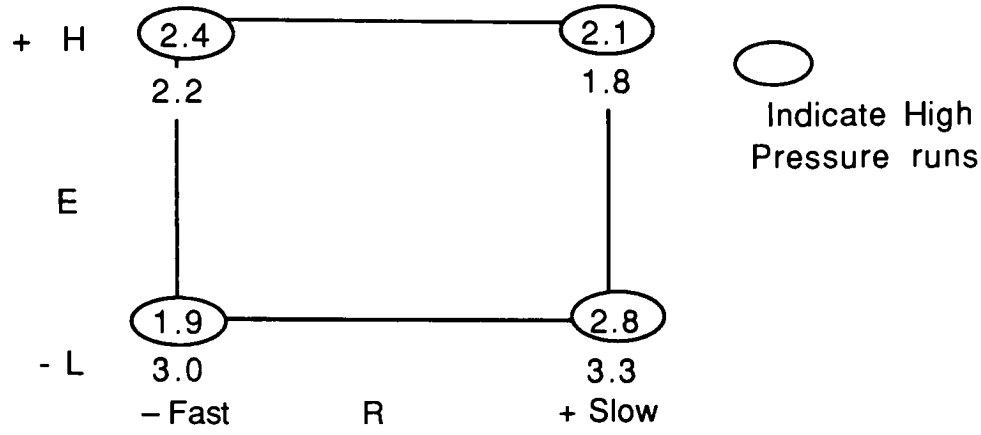

Figure 15 Two-way table for discussing ER interaction effect. This is a projection of one of the cubes in Figure 14 onto a plane containing only E and R. The numbers are the refractive indices.

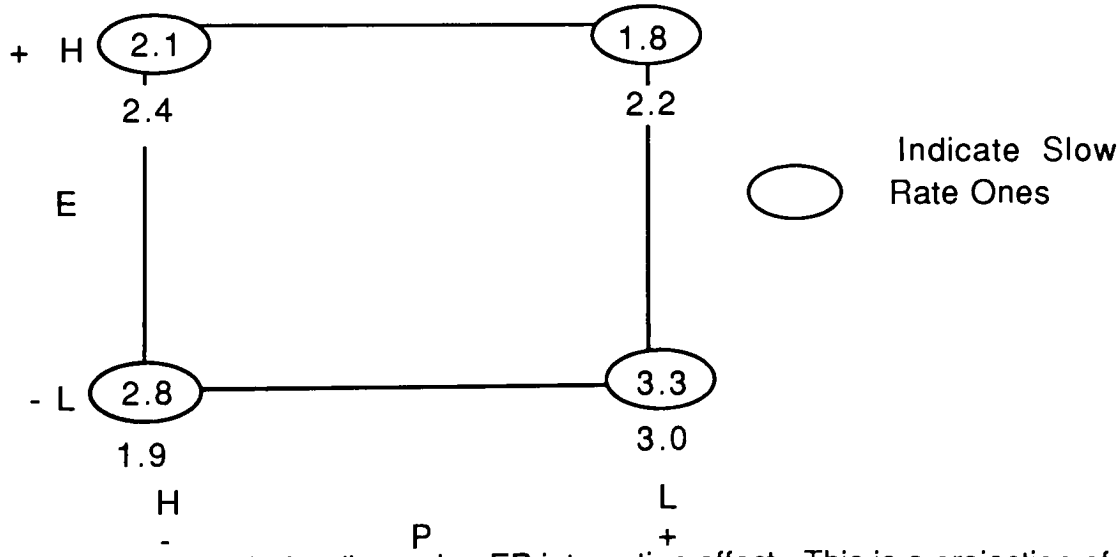

Figure 16 Two way table for discussing EP interaction effect. This is a projection of one of the cubes in Figure 14 onto a plane containing only E and P. The numbers are the refractive indices.

In Figure 16 the projection is onto the E-P plane. Both the best (low n—1.8, 2.1) and worst (high n—3.3, 3.0) conditions occur at low pressure. At low pressure, n decreased with increased electrical biasing; while at high pressure no trend is seen. Again this indicates an interaction between the two variables

2. Second Designed Factorial Experiment

Based on the results above, a second experiment was designed. In this experiment, films were first deposited onto glass slides and then onto silicon wafers in order to get refractive index readings from both the spectrophotometer and the ellipsometer. The ellipsometer results were ambiguous and so will not be discussed in detail.

Chamber pressures were 2.0×10^{-4} Torr and 2.0×10^{-5} Torr, as in the first experiment. More accurate tooling factors were obtained from the first experiment, so that the deposition rate was better controlled. Rates were 11 Å/sec and 5 Å/sec. The bias voltages were 100 V and 500 V. The range of bias voltage was reduced to check out if the strong bias effect of the first experiment is partly caused by the large range of voltage. The conditions of the second experiment are illustrated in Table 10.

Table 10 The conditions of second experiment on glass slides.

Sample	Bias (V)	R (Å/sec)	P (Torr)
1, 9	100	10.03, 8.67	2.0×10^{-4}
2	500	9.82	2.0×10^{-4}
3	100	4.32	2.0×10^{-4}
4, 10	500	5.55, 5.67	2.0×10^{-4}
5	100	11.04	2.0×10^{-5}
6, 11	500	9.10, 10.51	2.0×10^{-5}
7, 12	100	4.61, 5.39	2.0×10^{-5}
8	500	5.09	2.0×10^{-5}

Table 11 The second experiment on glass slides (2^3 conditions). Here pressure, rate, and biasing voltage were varied but temperature was fixed at 150°C.

	Bias (V)	Rate	Pressure
−	100	fast	high
+	500	slow	low

N	Run	E	R	P	n	Ave n	DOF	Effect	
1	B3	-	F	H	3.69	3.45	8	Ave	3.134
2	C4	+	F	H	3.55	3.55	4	E	**0.403**
3	A2	-	S	H	1.57	1.57	4	R	**-0.387**
4	C3	+	S	H	2.10	2.70	4	ER	-0.023
5	A4		F	L	2.78	2.78	4	P	**0.633**
6	A3	+	F	L	3.68	3.53	4	EP	-0.213
7	C1	-	S	L	4.16	3.93	4	RP	**0.978**
8	B1	+	S	L	3.56	3.56	4	ERP	**-0.538**
9=1	C2	-	-	-	3.21				
10=4	A1	+	+	-	3.30	Estimate of standard error s = 0.496			
11=6	B2	+	-	+	3.38				
12=7	B4	-	+	+	3.70				

From the results in Table 11 we can make some conclusions. The estimate of standard error was calculated as s = 0.496.

(1) The pressure effect was very significant. The effect of biasing voltage and rate were smaller and may be insignificant since they are less than the standard error. Thus it appears that a presence of a bias voltage greater than 100 V has litttle effect on n. The first experiment however established the need for a non-zero bias voltage.

(2) The RP interaction is very significant. Low rate and high pressure are desirable for low refractive index films. This can be seen in Figure 17 where the data cube is projected onto the RP plane. At high pressure, rate appears to have a pronounced effect on the index, while at low pressure rate has little effect. Likewise, at slow rates, pressure has an effect, but at fast rates it does not. Bias level has a major effect only when the rate is slow and the pressure is high.

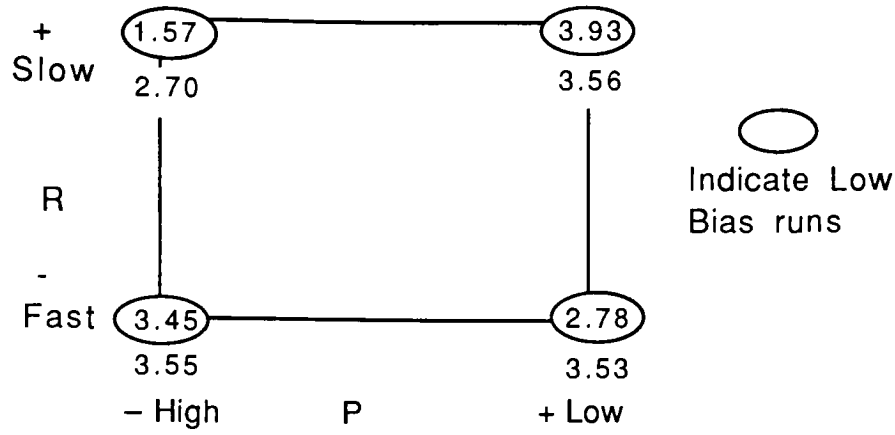

Figure 17 Two-way table for discussing the RP interaction.

(3) The three way ERP interaction appears significant, probably because of the large standard error, s.

(4) Other effects are negligible compared to s.

The four samples produced under high pressure have a lower refractive index than those produced under low pressure. This suggests that high pressure is more ideal for the growth of low index films because the amount of oxygen in the chamber is more and the chance that oxygen can impinge on substrate is higher.

A subset of the four high pressure coatings (P = 2.0 x 10^{-4} Torr) with are only two variables, E and R was done. The results are in Table 12. At high pressure, rate has a very significant effect on film refractive index with lower rates leading to smaller refractive indices. This confirms the conclusion earlier reached when considering the RP interaction .

The effects of bias, E, and the interaction, ER, are also significant, but have less of an effect on the refractive index.

Table 12 High pressure subset of the second experiment on glass slides.

E	R	Index n	DOF	Effect	
Low	Fast	3.45	4	Ave	2.8175
Hi	Fast	3.55	2	E	0.615
Low	Slow	1.57	2	R	-1.365
Hi	Slow	2.70	2	ER	0.515

The same experiment was repeated with silicon wafer substrates. Refractive index readings were obtained from the ellipsometer which used a fixed wavelength of 632.8 nm. A computer was interfaced to the ellipsometer to collect data and to analyze the results. The program used was designed only for transparent films having no absorption. Since many of the films produced had some silicon remaining in them, some absorption was expected. The values of n obtained from the ellipsometer were considerably different from the indices obtained from the spectrophotometer, however, a statistical analysis of the data gave similar results. Due to the uncertainty in the ellipsometric results they are not reported on here.

Table 13 The visual appearance of second experiment—silicon wafer samples.

#	E	R	P	Appearance
1	-	-	-	Light Purple
9	-	-	-	Very Light Green
2	+	-	-	Light Green
13	+	-	-	Light Green
3	-	+	-	Green & Purple
14	-	+	-	Green & Purple
4	+	+	-	Green Yellow
10	+	+	-	Green Yellow
5	-	-	+	Light Grey
6	+	-	+	Light Grey
11	+	-	+	Light Grey
7	-	+	+	Transparent Grey
12	-	+	+	Transparent Grey
8	+	+	+	Light Green & Orange

Other evidence came from the appearance of films on silicon wafers. Table 13 gives the visual appearance of the second experiment on silicon wafer samples. Films produced under high pressure conditions look very light and bright, while films produced under low pressure condition usually look grey, somewhat like pure silicon. This phenomenon suggests that reactive evaporation is more likely at high chamber pressure.

3. Third Designed Factorial Experiment

A third experiment was designed to confirm the results of the first two experiments. In this experiment, the substrate temperature was 150°C, and the biasing voltage was 500 V. The deposition rate was controlled at high (>10Å/sec) and low (<5Å/sec) rates. Chamber pressures were 2.0×10^{-4} Torr and 1.0×10^{-4} Torr. Each condition of the 2^2 design was repeated, as indicated in Table 14. Films were deposited onto glass slides. High pressure, slow rate films looked very light yellow and had no maxima on the transmittance spectra from the spectrophotometer. In order to complete the analysis we assumed that the index must be similar to previously obtained indices, and these range from 1.5 to 2.1 to 2.7. Accordingly a statistical analysis was done with each of three possible values of the index. The three analyses are in Table 15.

Table 14 Conditions and results of the third experiment.

#	Pressure (Torr)	Dep. Rate (Å/sec.)	Refractive Index
C1	1.0×10^{-4}	10.48	3.55
D1	1.0×10^{-4}	13.87	4.44
C2	1.0×10^{-4}	4.07	2.73
D2	1.0×10^{-4}	2.84	2.47
C3	2.0×10^{-4}	16.46	2.9
D3	2.0×10^{-4}	11.27	2.25
F1	2.0×10^{-4}	x	Could not be
F2	2.0×10^{-4}	x	measured.

For all choices of the index for the high pressure, low deposition rate condition, P and R have very significant effect. At high chamber pressure and slow deposition rate, the film refractive index is low. The PR interaction effect may or may not be significant depending on the choice of the unmeasurable index.

Table 15 The results and analysis for third experiment. As discussed in the text the analysis was repeated for three possible values of the unavailable indices. This varied rate and pressure. Bias was 500 V and substrate temperature was 150°C.

Pressure	Rate	n	dof		Effect
L	F	4	4	Ave	2.82
L	S	2.6	2	R	-0.94
H	F	2.58	2	P	-0.96
H	S	2.1	2	RP	0.46
P	R	Estimate of s =		0.33	

Pressure	Rate	n	dof		Effect
L	F	4	4	Ave	2.97
L	S	2.6	2	R	-0.64
H	F	2.58	2	P	-0.66
H	S	2.7	2	RP	0.76

Pressure	Rate	n	dof		Effect
L	F	4	4	Ave	2.67
L	S	2.6	2	R	-1.24
H	F	2.58	2	P	-1.26
H	S	1.5	2	RP	0.16

Two depositions with different conditions were made onto sodium chloride so that the film composition might be inspected with FTIR. In both cases T_{sub} = 150°C, P_{cham} = 2.0 x 10^{-4} Torr, and bias = 500 V. The first deposition rate was less than 5Å/sec and the second rate was greater than 10Å/sec. The FTIR spectra are in Figures 19 and 20, and the compositions are in Tables 16 and 17.

Table 16 The composition of silicon oxide film deposited under T_{sub} =150°C, P_{cham} = 2.0 x 10^{-4} Torr, Bias = 500 Volt, and deposition rate < 5Å/sec.

Name of Bond	Wavenumber(cm-1)	Exist
Aliphatic C-H Bond, Stretch	2900 ~ 3000	Yes
Si-O	~ 1000	Yes

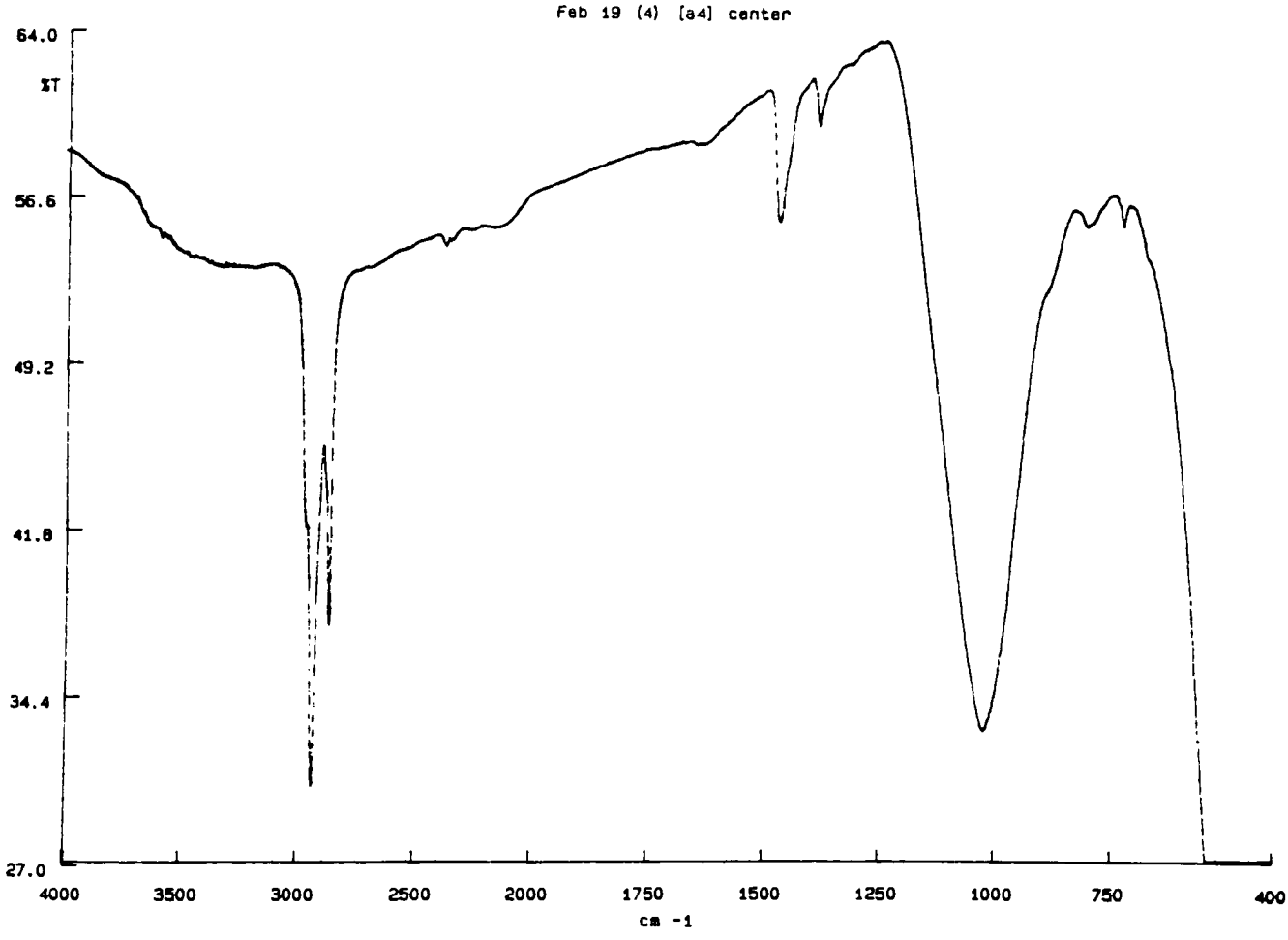

Figure 18 The IR spectrum for silicon oxide film deposited under T_{sub} = 150°C, P_{cham} = 2.0 x 10^{-4} Torr, bias = 500 V, and deposition rate < 5Å/sec.

Table 17 The composition of silicon oxide film deposited under T_{sub} =150°C, P_{cham} = 2.0 x 10^{-4} Torr, bias = 500 Volt, and deposition rate <10Å/sec.

Name of Bond	Wavenumber(cm-1)	Exist
Aliphatic C-H Bond, Stretch	2900 ~ 3000	No
Si-O	~ 1000	Yes

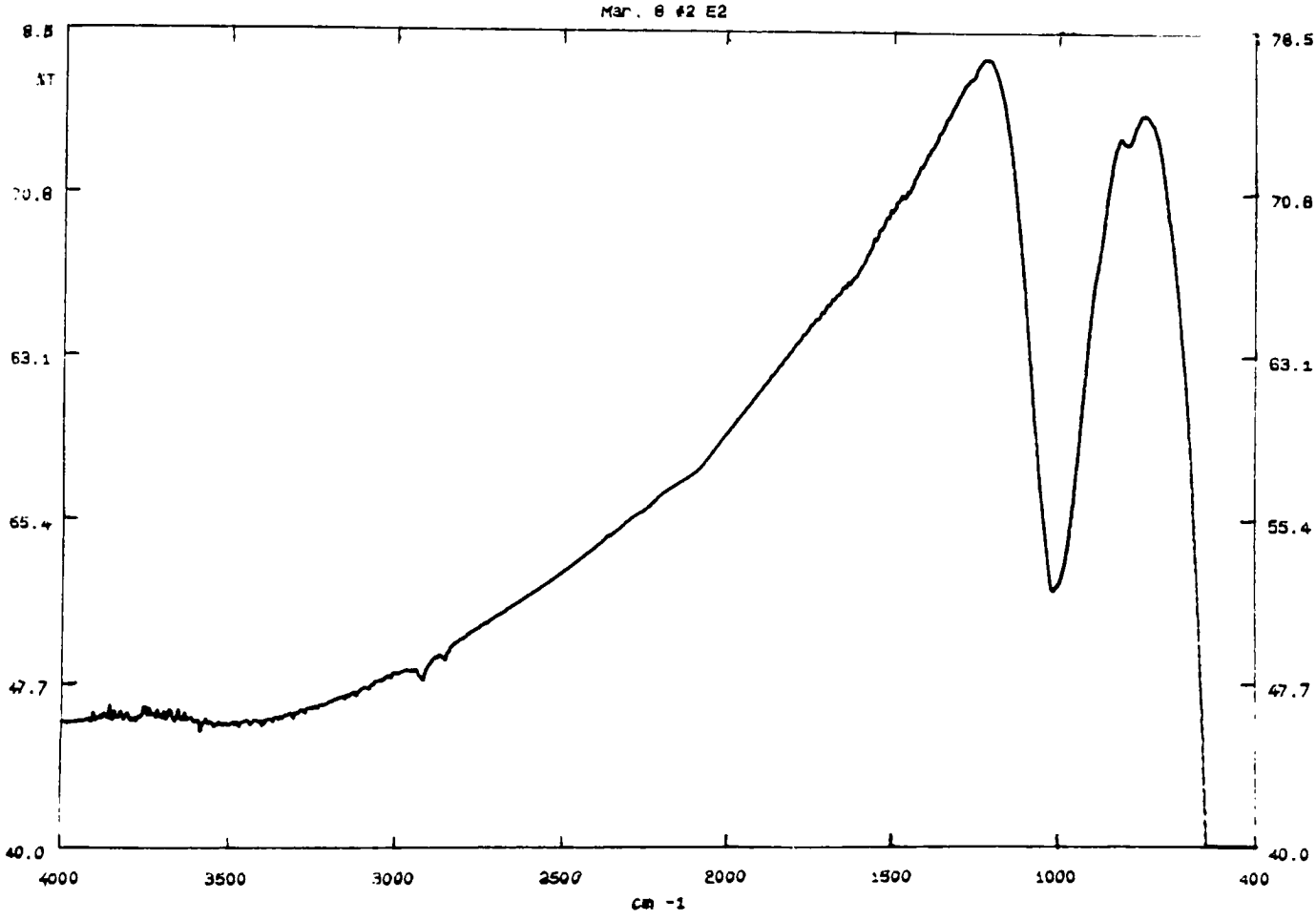

Figure 19 The IR spectrum for silicon oxide film deposited under T_{sub} =150°C, P_{cham} = 2.0 x 10^{-4} Torr, bias = 500 Volt, and deposition rate <10Å/sec.

From the FTIR results on pure silicon films, Table 4, it can be understood that neither Si-O nor C-H bonds exist. In the other words, the film is pure silicon with no silicon oxides. In Table 16 and Table 17, Si-O bonds exist on the spectrum of both films, meaning silicon oxides did form under these two specific conditions. In Table 16, the aliphatic C-H bond stretch was probably caused by the contamination of the film by pump oil.

V. Conclusion

VA. First Experiment

The first experiment had sixteen (2^4) conditions with two values each of four variables.

(1) Temperature had a strong effect. For higher substrate temperatures, the atoms on the surface will have more energy meaning greater mobility and more chance to find a low energy final site, in many cases as SiO_x. The increase in temperature should also increase the reaction rate. Main effects of bias, rate, and pressure appeared to be important. Later analysis with only high temperature slides proved this point. The main effects may have been statistically small since low temperature data had a large amount of variation.

(2) Large three-way interactions probably came from large variance in the data.

VB. Second Experiment

The second experiment had eight(2^3) conditions with three variables with high substrate temperature.

(1) Pressure was determined as the most important factor. At high pressures, rate was very important. Generally speaking, high pressure, low rate conditions are most ideal for low refractive index films. This probably is because at high pressure and low rate there is an ample amount of oxygen for each silicon that deposits, meaning a SiO_x deposition of low index.

(2) The effect of biasing was not simple. An increase in biasing voltage sometimes increased n, and sometimes decreased it. The lowest index occured for

films deposited at high pressure, low rate, and high bias.

(3) The PR effect could be important because it's the interaction of two important factors. EP and ER interactions should be less important. This suggests an interaction between variables.

VC. Third Experiment

The third experiment had only four conditions. Temperature was fixed at 150°C, and biasing voltage was 500 V.

(1) Both pressure and rate will had an important effect on the film refractive index.

(2) The PR interaction was of marginal importance.

(3) For the lowest refractive index, the rate must be as low as possible, the pressure must be high, and biasing must exist. The level of biasing has little effect on the film refractive index.

Conclusions based on all results are:

(1) High temperature conditions will give us low refractive indices.

(2) Chamber pressure and deposition rate are both very significant for changing film refractive indices. High chamber pressure and low deposition rate will produce low refractive index film.

(3) Biasing at some level is needed and for the lowest index should be large.

VD. Evaluation

The results I have obtained sometimes have large standard error and are not as valuable as expected. Even though the final purpose is to apply silicon and silicon related films on multilayer devices, further research is needed to work out some problems. Below are some points which I believe should be improved to achieve better results and increase the probability of applications.

(1) The results sometimes have large variation under the same conditions. This variation occurs partly from the instruments and partly from the personnel operation. The crystal inside the rate monitor should be changed as frequently as possible. The more time it has been used, the less accurate it is. The hot tungsten filament had contamination problems, which caused unstable electric current. On the other hand, dexterous experimental skill is required because several variables must be controlled at the same time.

(2) A considerable amount of variation may arise from the method which was used to obtain the refractive index with the spectrophotometer. Since the films were not uniform, thickness measurements at several locations on each film were taken and averaged. The beam from the spectrophotometer struck the film over an area. The question is will the average thickness be close to the actual thickness in the incident area? How much deviation does the average thickness have in comparison with the actual thickness? A large variation in thickness will lead to a less accurate measure of the refractive index.

(3) Only Fourier Transform Infrared Spectrophotometer was used to determine the composition of films. It provided only qualitative, non-detailed information such as the presence or absence of a silicon-oxide bond. A more powerful method, such as XPS, should be employed to tell the actual composition since the content of silicon oxide has important effect on film refractive index.

VI. References

1. " Optical Thin Films : User's Handbook", James D. Rancourt, Macmillan Publishing Company, New York, (1987).

2. " Optics", Eugene Hecht, Second Edition, Addison-Wesley Publishing Company, Inc., (1987).

3. " Optics", F.G. Smith, John Wiley & Sons Ltd., (1988).

4. " Concepts of Classical Optics", John Strong, W.H. Freeman & Company, (1958).

5. " Optics", Miles V. Klein and Thomas E. Furtak, 2nd Edition, John Wiley & Sons, Inc., (1986).

6. " Optics : A Short Course for Engineers and Scientists", Charles S. Williams and Orville A. Becklund, Wiley Interscience, (1972).

7. " Optics", Arnold Sommerfeld, Academic Press Inc., Publishers, (1964).

8. " Thin Film Device Applications", Kasturi Lal Chopra and Inderjeet Kaur, Plenum Press, New York, (1983).

9. " Influence of Ion Assistance on The Optical Properties of MgF_2", Philip J. Martin, Wayne G. Sainty, Roger P. Netterfield, David R. Mckenzie, David J. H. Cockayne, Soey H. Sie, Obert R. Wood and Harold G. Craighead, Applied Optics, Vol. 26, No. 7, p. 1235 (1987).

10. " Porous Fluoride Antireflective Coatings", Ian M. Thomas, Applied Optics, Vol. 27, No. 16, p. 3356 (1988).

11. " Broadband Reflectance Coatings for Vacuum Ultraviolet Application" Howard Herzig, B. K. Flint., C. M. Fleetwood, Jr., Applied Optics, Vol. 26, No. 4, p. 605 (1987).

12. " Inhomogenity of the Refractive Index of ZnS Film", Qihong Wu, Applied Optics, Vol. 26, No. 18, p. 3753 (1987).

13. " No Visible Electrochromism in High-Quality E-Beam Evaporated In_2O_3 : Sn Films", J. S. E. M. Svensson and C. G. Granqvist, Applied Optics, Vol. 24, No. 15, p. 2284 (1985).

14. " Transparent and Infrared-Reflecting Indium-Tin-Oxide Films: Quantitative Modeling of The Optical Properties", Ivar Hamberg and Claes G. Granqvist, Applied Optics, Vol. 24, No. 12, p. 1815 (1985).

15. " Comparison of the Properties of Titanium Dioxide Films Prepared By Various Techniques", J. M. Bennett, Emile Pelletier, G. Albrand, J. P. Borgogno, B. Lazaarides, Charles K. Carniglia, R.A. Schmell, Thomas. H. Allen, Turdy Tuttle-Hart, Karl H. Guenther and Andeas Saxer, Applied Optics, Vol. 28, No. 15, p. 3303 (1989).

16. " Raman Characterization of All-Dielectric Multilayer SiO_2/ TiO_2 Optical Coatings", Gregory J. Exarhos and Walter T. Pawlewicz, Applied Optics, Vol. 23, No. 12, p. 1986 (1984).

17. " Optically Transparent IR Reflective Heat Mirror Films of ZnS-Ag-ZnS", Bruce W. Smith, Master's Thesis of Rochester Institute of Technology, (1989).

18. " Handbook of Optical Constants of Solids", Edward D. Palik, Academic Press Inc., (1985).

19. " Formation of Silicon Nitride Films Newly Developed by the Ion and Vapour Deposition Method", F. Sugawara, T. Ajioka, F. Ichikawa and S. Ushio, Mat. Soc. Symp. Proc., **54**, 535 (1986).

20. " Electrical and Optical Properties of Amorphous Si_xN_{1-x}". B. Dunnett, D. I. Jones and A. D. Stewart, Philosophical Magazine B, Vol. 53, No. 2, p. 159-169 (1986).

21. " Characterization of Oxygen-Doped, Plasma-Deposited Silicon Nitride", W. R. Knolle and J. W. Osenbach, J. Electrochem. Soc. : Solid-State Science And Technology, Vol. 135, No. 5, p. 1211 (1989).

22. " Formation of Thin Silicon Oxide Films by Rapid Thermal Heating", J. P. Ponpon, J. J. Grob, A. Grob and R. Stuck, J. Appl. Phys. 59 (11), p. 3921(1986).

23. " Infrared Optical Properties of Electron-Beam Evaporated Silicon Oxynitride Films", T. S. Eriksson and C. G. Granqvist, Applied Optics, Vol. 22, No. 20, p. 3204 (1983).

24. " Low Temperature Plasma Chemical Vapor Deposition of Silicon Oxynitride Thin-Film Waveguides", D. K. W. Lam, Applied Optics, Vol. 23, No.16, p. 2744 (1984).

25. "Microstructure Analysis of Thin Films Deposited by Reactive Evaporation and by Reactive Ion-Plating", Karl H. Guenther, Boon Loo, David Burns, Jo Edgell, Debbie Winndham and Karl-Heinz Muller, Thin Film Technology III, Vol. 1019, p. 73 (1988).

26. " Optical Films Deposited by A Reactive Ion Plating Process", H. K. Pulker, M. Buhler and R. Hora, Optical Thin Films II, Vol. 678, p. 110 (1986).

27. "Statistics for Experiments: An Introduction to Design, Data Analysis and Model Building", George E.P. Box, William G. Hunter, J. Stuart Hunter, John Wiley & Sons (1978).

VII. Appendices

VII.1 Analysis of a 2^4 Full Factorial Experiment

This shows the methods of calculating the effects in a 2^4 Factorial Experiment. As mentioned in Section IV.A, two values of each of the four variables are chosen and a sample is produced for all possible combinations of variables. The n_i represent the index of refraction measured at each of the 16 experimental conditions. Effects are calculated by the following formulae[27] and compared to an estimate of the standard error. Effects which exceed the standard error are deemed significant. The results are shown in Table 8. Similiar formulae hold for 2^3 and 2^2 experiments.

$$E \text{ main effect} = [\,(n_2-n_1)+(n_4-n_3)+(n_6-n_5)+(n_8-n_7)+(n_{10}-n_9)+(n_{12}-n_1) +(n_{14}-n_{13})+(n_{16}-n_{15})]\,/\,8$$

$$R \text{ main effect} = [\,(n_3-n_1)+(n_4-n_2)+(n_7-n_5)+(n_8-n_6)+(n_{11}-n_9)+(n_{12}-n_{10}) +(n_{15}-n_{13})+(n_{16}-n_{14})]\,/\,8$$

$$P \text{ main effect} = [\,(n_5-n_1)+(n_6-n_2)+(n_7-n_3)+(n_8-n_4)+(n_{13}-n_9)+(n_{14}-n_{10}) +(n_{15}-n_{11})+(n_{16}-n_{12})\,/\,8$$

$$T \text{ main effect} = [\,(n_9-n_1)+(n_{10}-n_2)+(n_{11}-n_3)+(n_{12}-n_4)+(n_{13}-n_5)+(n_{14}-n_6) +(n_{15}-n_7)+(n_{16}-n_8)\,/\,8$$

$$ER \text{ interaction effect} = 1/2\{\,[(n_4-n_3)-(n_2-n_1)]+[(n_8-n_7)-(n_6-n_5)] +[(n_{12}-n_{11})-(n_{10}-n_9)]+[(n_{16}-n_{15})-(n_{14}-n_{13})\}\,/\,4$$

$$EP \text{ interaction effect} = 1/2\{\,[(n_6-n_5)-(n_2-n_1)]+[(n_8-n_7)-(n_4-n_3)] +[(n_{14}-n_{13})-(n_{10}-n_9)]+[(n_{16}-n_{15})-(n_{14}-n_{13})]\,\}\,/\,4$$

ET interaction effect = $1/2\{ [(n_{10}-n_9)-(n_2-n_1)]+[(n_{12}-n_{11})-(n_4-n_3)]+[(n_{14}-n_{13})-(n_6-n_5)]+[(n_{16}-n_{15})-(n_8-n_7)] \} / 4$

RP interaction effect = $1/2\{ [(n_7-n_5)-(n_3-n_1)]+[(n_8-n_6)-(n_4-n_2)]+[(n_{15}-n_{13})-(n_{11}-n_9)]+[(n_{16}-n_{14})-(n_{12}-n_{10})] \} / 4$

RT interaction effect = $1/2\{ [(n_{11}-n_9)-(n_3-n_1)]+[(n_{12}-n_{10})-(n_4-n_2)]+[(n_{15}-n_{13})-(n_7-n_5)]+[(n_{16}-n_{14})-(n_8-n_6)] \} / 4$

PT interaction effect = $1/2\{ [(n_{13}-n_9)-(n_5-n_1)]+[(n_{14}-n_{10})-(n_6-n_2)]+[(n_{15}-n_{11})-(n_7-n_3)]+[(n_{16}-n_{12})-(n_8-n_4)] \} / 4$

ERP interaction effect = $1/2\{1/2[(n_8-n_7)-(n_6-n_5)]-1/2[(n_4-n_3)-(n_2-n_1)] \}$
$+1/2\{1/2[(n_{16}-n_{15})-(n_{14}-n_{13})]-1/2[(n_{12}-n_{11})-$
$-(n_{10}n_9)] \} / 2$

ERT interaction effect = $1/2\{1/2[(n_{16}-n_{15})-(n_{14}-n_{13})]-1/2[(n_8-n_7)-(n_6-n_5)] \}$
$+1/2\{1/2[(n_{12}-n_{11})-(n_{10}-n_9)]-1/2[(n_4-n_3)-$
$-(n_2-n_1)] \} / 2$

EPT interaction effect = $1/2\{1/2[(n_{16}-n_{15})-(n_{12}-n_{11})]-1/2[(n_8-n_7)-(n_4-n_3)] \}$
$+1/2\{1/2[(n_{14}-n_{13})-(n_{10}-n_9)]-1/2[(n_6-n_5)-$
$-(n_2-n_1)] \} / 2$

RPT interaction effect = $1/2\{1/2[(n_{16}-n_{14})-(n_{12}-n_{10})]-1/2[(n_8-n_6)-(n_4-n_2)] \}$
$+1/2\{1/2[(n_{15}-n_{13})-(n_{11}-n_9)]-1/2[(n_7-n_5)-$
$-(n_3-n_1)] \} / 2$

ERPT interaction effect = $1/2\{1/2[(n_{16}-n_{15})-(n_{14}-n_{13})]-1/2[(n_{12}-n_{11})$
$-(n_{10}-n_2)]\}-1/2\{1/2[(n_8-n_7)-(n_6-n_5)]$
$-1/2[(n_4-n_3)-(n_2-n_1)]\}/2$

VII.2. Other Methods of Computing the Effects

Calculation of the effects outlined in Appendix VII.1 can be done more simply by the use of Yate's Algorithm. Each of the two levels of a variable is assigned a sign, + or -. The signs of the interactions are the product of the signs of the variables (sign of ER = [sign of E x sign of R]), as shown in Table 8. To get the value of an effect, one multiplies the sign from Table 8 by the index of refraction at that combination of variables. By inspecting the table one can see that this results in the same formulae as in the previous section.

Table 18 Signs for calculating effects of first set experiment (2^4 conditions).

Ave.	E	R	P	T	ER	EP	ET	RP	RT	PT	ERP	ERT	EPT	RPT	ERPT	n
+	-	-	-	-	+	+	+	+	+	+	-	-	-	-	+	3.15
+	+	-	-	-	-	-	-	+	+	+	+	+	+	-	-	2.68
+	-	+	-	-	-	+	+	-	-	+	+	+	-	+	-	2.86
+	+	+	-	-	+	-	-	-	-	+	-	-	+	+	+	2.4
+	-	-	+	-	+	-	+	-	+	-	+	-	+	+	-	2.13
+	+	-	+	-	-	+	-	-	+	-	-	+	-	+	+	3.25
+	-	+	+	-	-	-	+	+	-	-	-	+	+	-	+	2.37
+	+	+	+	-	+	+	-	+	-	-	+	-	-	-	-	3.47
+	-	-	-	+	+	+	-	+	-	-	-	+	+	+	-	1.9
+	+	-	-	+	-	-	+	+	-	-	+	-	-	+	+	2.39
+	-	+	-	+	-	+	-	-	+	-	+	-	+	-	+	2.76
+	+	+	-	+	+	-	+	-	+	-	-	+	-	-	-	2.11
+	-	-	+	+	+	-	-	-	-	+	+	+	-	-	+	2.98
+	+	-	+	+	-	+	+	-	-	+	-	-	+	-	-	2.24
+	-	+	+	+	-	-	-	+	+	+	-	-	-	+	-	3.34
+	+	+	+	+	+	+	+	+	+	+	+	+	+	+	+	1.83
16	8	8	8	8	8	8	8	8	8	8	8	8	8	8	8	Divisor

Yates's Algorithm gives a means of automating the calculations so that they can be easily done in a spreadsheet. Tables 9 and 10 show the algorithm. The solid lines

in Table 9 indicate addition of two indices while the dashed lines indicate subtraction, second value minus first value. Thus in row 1, column Y1 of Table 10, 5.83 = 3.15 + 2.68; likewise for row 16, column Y1, -1.51 = 1.83 - 3.34. Repeating this algorithm three more times yields column Y4. Dividing Y4 by the degrees of freedom gives the value of the effect. As is shown in Reference 27, this gives the same results as in the previous section.

Table 19 The easy way to calculate effects of first set experiment[27] (2^4 conditions).

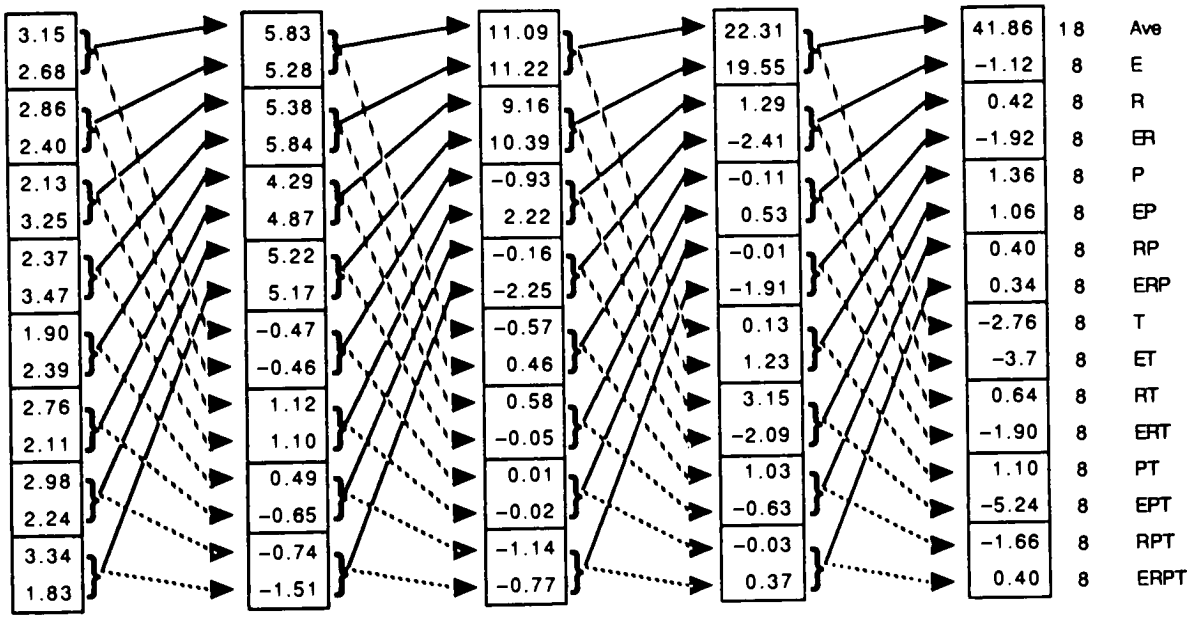

Table 20 Statistics on the effects for the first experiment with 2^4 conditions[27].

N	E	R	P	T	Index	Y 1	Y 2	Y 3	Y 4	Dof		Effects
1	-	-	-	-	3.15	5.83	11.09	22.31	41.86	16	Ave	2.616
2	+	-	-	-	2.68	5.26	11.22	19.55	-1.12	8	E	-0.140
3	-	+	-	-	2.86	5.38	9.16	1.29	0.42	8	R	0.053
4	+	+	-	-	2.40	5.84	-10.39	-2.41	-1.92	8	ER	-0.240
5	-	-	+	-	2.13	4.29	-0.93	-0.11	1.36	8	P	0.170
6	+	-	+	-	3.25	4.87	2.22	0.53	1.06	8	EP	0.133
7	-	+	+	-	2.37	5.22	-0.16	-0.01	0.40	8	RP	0.050
8	+	+	+	-	3.47	5.17	-2.25	-1.91	0.34	8	ERP	0.043
9	-	-	-	+	1.90	-0.47	-0.57	0.13	-2.76	8	T	**-0.345**
10	+	-	-	+	2.39	-0.46	0.46	1.23	-3.70	8	ET	**-0.463**
11	-	+	-	+	2.76	1.12	0.58	3.15	0.64	8	RT	0.080
12	+	+	-	+	2.11	1.10	-0.05	-2.09	-1.90	8	ERT	-0.238
13	-	-	+	+	2.98	0.49	0.01	1.03	1.10	8	PT	0.138
14	+	-	+	+	2.24	-0.65	-0.020	-0.63	-5.24	8	EPT	**-0.655**
15	-	+	+	+	3.34	-0.74	-1.14	-0.03	-1.66	8	RPT	-0.208
16	+	+	+	+	1.83	-1.51	-0.77	0.37	0.40	8	ERPT	0.050

-	0	Fast rate	High pressure	Cold	Estimate of s = 0.326
+	500	Slow rate	Low pressure	Hot	